

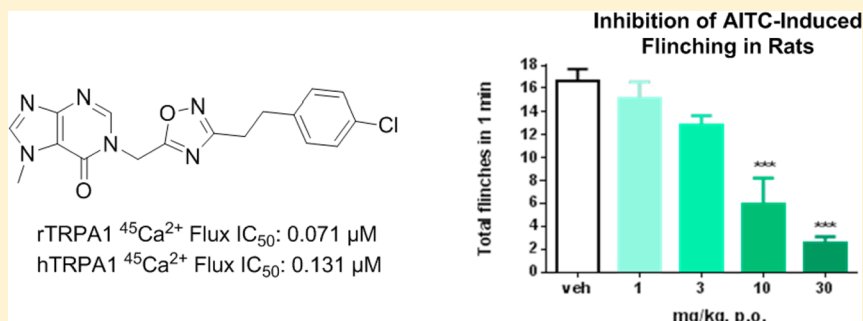
Optimization of a Novel Quinazolinone-Based Series of Transient Receptor Potential A1 (TRPA1) Antagonists Demonstrating Potent *In Vivo* Activity

Laurie B. Schenkel,^{*,†} Philip R. Olivieri,[†] Alessandro A. Boezio,[†] Holly L. Deak,[†] Renee Emkey,[‡] Russell F. Graceffa,[†] Hakan Gunaydin,[§] Angel Guzman-Perez,[†] Josie H. Lee,[‡] Yohannes Teffera,^{||} Weiya Wang,[⊥] Beth D. Youngblood,[⊥] Violeta L. Yu,[‡] Maosheng Zhang,[⊥] Narender R. Gavva,[⊥] Sonya G. Lehto,[⊥] and Stephanie Geuns-Meyer[†]

[†]Departments of Medicinal Chemistry, [‡]Lead Discovery, [§]Molecular Structure, and ^{||}Pharmacokinetics and Drug Metabolism, Amgen, Inc., 360 Binney Street, Cambridge, Massachusetts 02142, United States

[⊥]Neuroscience, Amgen, Inc., One Amgen Center Drive, Thousand Oaks, California 91320, United States

S Supporting Information



ABSTRACT: There has been significant interest in developing a transient receptor potential A1 (TRPA1) antagonist for the treatment of pain due to a wealth of data implicating its role in pain pathways. Despite this, identification of a potent small molecule tool possessing pharmacokinetic properties allowing for robust *in vivo* target coverage has been challenging. Here we describe the optimization of a potent, selective series of quinazolinone-based TRPA1 antagonists. High-throughput screening identified 4, which possessed promising potency and selectivity. A strategy focused on optimizing potency while increasing polarity in order to improve intrinsic clearance culminated with the discovery of purinone 27 (AM-0902), which is a potent, selective antagonist of TRPA1 with pharmacokinetic properties allowing for >30-fold coverage of the rat TRPA1 IC₅₀ *in vivo*. Compound 27 demonstrated dose-dependent inhibition of AITC-induced flinching in rats, validating its utility as a tool for interrogating the role of TRPA1 in *in vivo* pain models.

■ INTRODUCTION

TRPA1 is a nonselective cation channel and member of the transient receptor potential (TRP) superfamily of ion channels. TRPA1 is highly expressed in sensory neurons of the dorsal root ganglia and is activated by a range of irritants. Reactive electrophiles such as allyl isothiocyanate (AITC), allicin, and cinnamaldehyde, the pungent components of mustard oil, garlic, and cinnamon, respectively, activate the channel via covalent modification of cysteine residues and elicit a painful response in humans.¹ Sensory neurons from TRPA1-deficient mice show diminished response to these types of irritants, which strongly supports the role of TRPA1 in mediating their pain response.² TRPA1 can also be activated via noncovalent mechanisms, including exposure to unreactive small molecules such as gingerol³ and thymol,⁴ inflammatory peptides,⁵ cold temperature,² and mechanical force.⁶

A number of preclinical studies provide additional support for the role of TRPA1 in pain. TRPA1 knockout mice demonstrate significantly diminished flinching behavior upon exposure to the selective agonist AITC,² as well as to formalin⁷ and the inflammatory mediator 4-hydroxynonenal.⁸ Knockout mice also respond less to the application of tactile force.⁶ Pharmacological blockade of TRPA1 with antagonists, such as xanthine HC-030031 (1)⁹ and oxime AP-18 (2),¹⁰ have shown efficacy in formalin- and complete Freund's adjuvant (CFA)-induced models of inflammatory pain and the spinal nerve ligation (SNL) model of neuropathic pain (Figure 1). While these results demonstrate the potential utility of treating pain with small molecule TRPA1 antagonists, the weak potencies (3–10 μM) and/or poor pharmacokinetic properties of these

Received: January 8, 2016

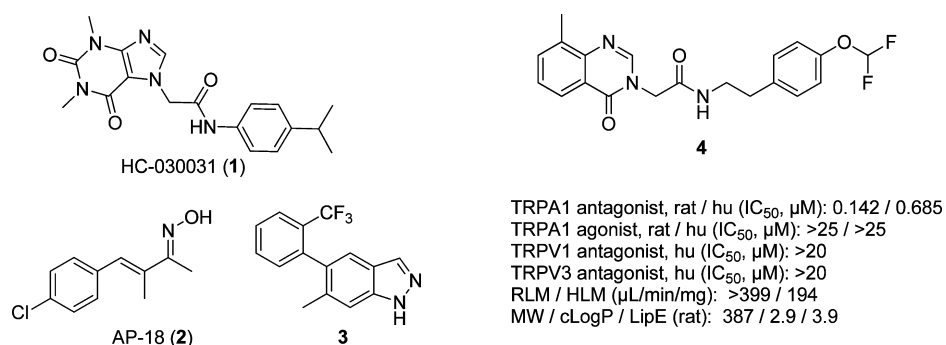


Figure 1. Previously reported TRPA1 antagonists and profile of HTS hit 4.

Table 1. SAR of the Quinazolinone Amides^a

compd	R	R ¹	rTRPA1 IC_{50} (μM) ^b	hTRPA1 IC_{50} (μM) ^b	RLM/HLM $Cl_{int, app}$ ($\mu L/min/mg$) ^c	cLogP
4	8-Me	<i>p</i> -OCHF ₂	0.142	0.685	>399/194	2.9
5	8-Me	H	U ^{d,e}	>8.33 ^e	ND/ND	2.6
6	8-Me	<i>p</i> -OMe	1.37 ^e	U ^{d,e}	ND/ND	2.5
7	8-Me	<i>m</i> -OMe	>16.7 ^e	>16.7 ^e	ND/ND	2.5
8	8-Me	<i>o</i> -OMe	>16.7 ^e	>16.7 ^e	ND/ND	2.5
9	8-Me	<i>p</i> -Cl	0.358	0.802	706/224	3.3
10	H	<i>p</i> -Cl	U ^{d,e}	>16.7 ^e	104/31	2.8
11	7-Me	<i>p</i> -Cl	>16.7 ^e	>4.2 ^e	829/144	3.3
12	6-Me	<i>p</i> -Cl	0.287	0.265	ND/ND	3.3
13	5-Me	<i>p</i> -Cl	0.112	0.070	736/301	3.3
14	8-CF ₃	<i>p</i> -Cl	0.306 ^e	0.286 ^e	>399/397	3.7
15	8-F	<i>p</i> -Cl	0.791 ^e	1.33 ^e	186/40	2.9
16	8-OMe	<i>p</i> -Cl	2.15 ^e	1.46 ^e	455/34	3.0
17	8-CN	<i>p</i> -Cl	0.056	0.201	297/49	2.3
18	8-aza	<i>p</i> -Cl	1.17	1.18	18/<14	1.7
19	7-aza	<i>p</i> -Cl	1.08	1.71	179/14	1.7

^aData represent the mean of ≥ 2 independent dose–response curves, except where noted. Standard deviation values are provided in the [Supporting Information](#). ^bAntagonist IC_{50} , FLIPR assay. ^cND = not determined. ^dU = undefined; inhibition crossed the 50% threshold, but a curve could not be fit. ^eData represents $n = 1$ dose–response curve.

and other first generation antagonists make it challenging to assess whether the observed *in vivo* effects are truly mediated by TRPA1, as significant target coverage was difficult to achieve. A recently reported (trifluoromethylphenyl)indazole antagonist (3) showed good potency ($<0.1 \mu M$) against TRPA1 across species and good selectivity over other TRP channels (Figure 1).¹¹ Importantly, dose-dependent reversal of both CFA-induced mechanical hyperalgesia in rats and AITC-induced allodynia in mice was demonstrated upon oral dosing. However, broader selectivity against a range of off-targets and *in vivo* free drug concentrations were not reported.

The discovery of a human genetic link between TRPA1 and familial episodic pain syndrome provides still further evidence that TRPA1 plays a significant role in human pain.¹² Patients carrying a single gain-of-function mutation in TRPA1 experience debilitating bouts of upper body pain, triggered by some combination of fasting, cold, and fatigue. This data, combined with the numerous studies performed in rodents by either genetic or pharmacological knockdown of TRPA1, and the need for a potent, selective TRPA1 antagonist with pharmacokinetics enabling significant target coverage *in vivo*,

prompted us to initiate a program to identify such a compound. Here we report the discovery of a quinazolinone-based series of TRPA1 antagonists, optimization of which led to the identification of a compound possessing all of the features desired to evaluate the *in vivo* pharmacology of TRPA1.

RESULTS AND DISCUSSION

To validate the hypothesis that inhibition of TRPA1 is a suitable approach for the treatment of pain, we sought to identify a potent and selective tool compound that could provide good target coverage *in vivo* with oral dosing. High-throughput screening identified compound 4, which possessed submicromolar potency against both human and rat TRPA1 in a FLIPR Ca^{2+} imaging assay that measures inhibition upon activation with AITC (Figure 1). Compound 4 showed only antagonist activity and was inactive in agonist mode at concentrations up to $25 \mu M$. Despite its poor microsomal stability, 4 was an attractive hit based on its potency, selectivity against a small subset of other TRP channels, good physical properties, and a modular synthesis that would enable rapid analogue preparation and determination of SAR.

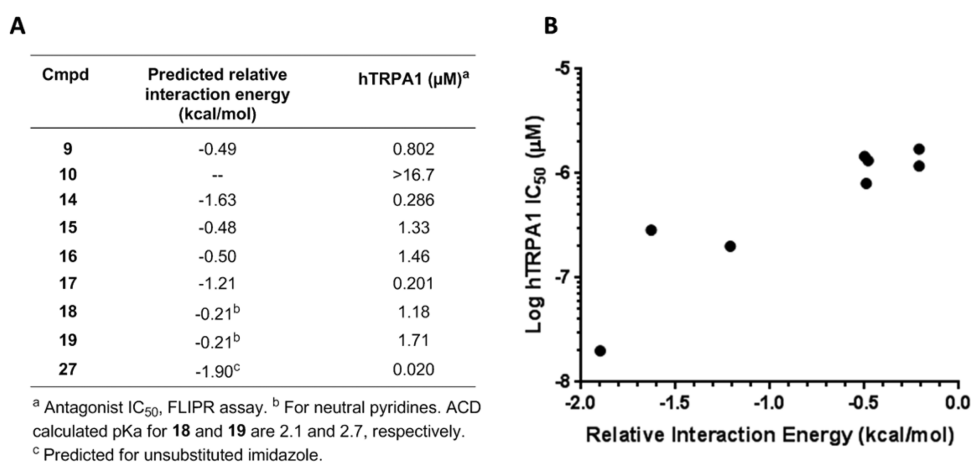


Figure 2. (A) Predicted relative interaction energies for a theoretical π -stacking interaction and measured human TRPA1 potencies. (B) Plot showing the correlation of the values in (A). Each point corresponds with a compound. Compound **10** is excluded.

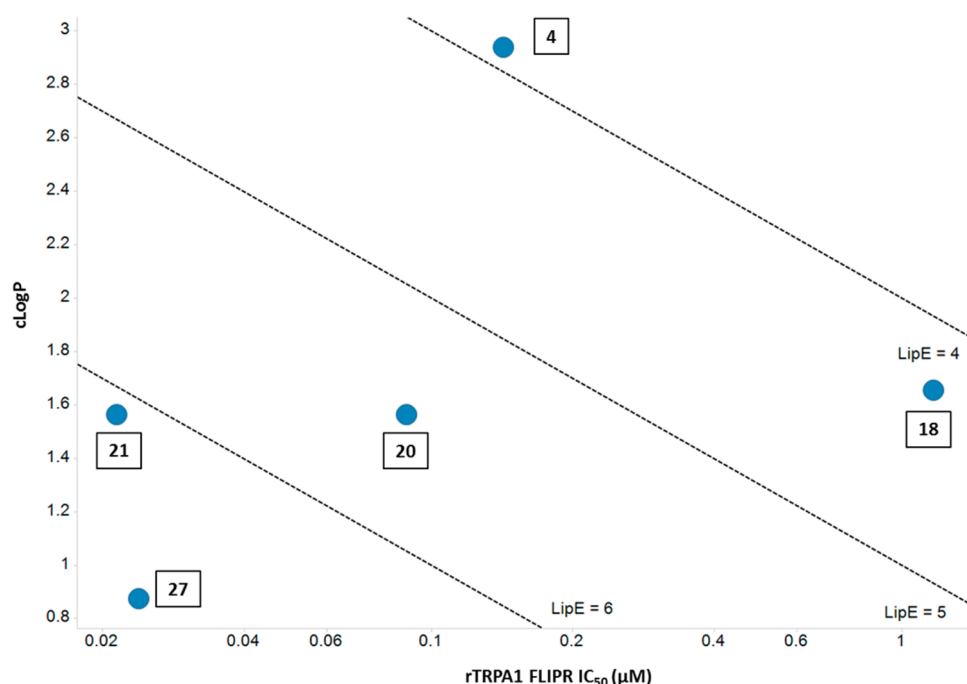


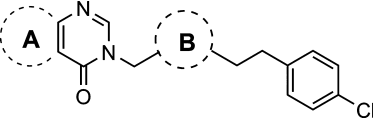
Figure 3. Plot demonstrating improvements in LipE for a subset of key compounds.

We first determined initial SAR around the phenyl ring (Table 1). Removal of the difluoromethoxy group was not well tolerated, as compound **5** lost significant activity. Seeking to find a potent, more readily available replacement for the difluoromethoxy moiety, we prepared compound **6**. However, replacement with a methoxy group also led to a loss of potency. Para-substitution was important for maintaining detectable activity in both species, as both **7** and **8** showed no inhibition at concentrations up to 16.7 μM . A scan of small substituents at the para-position identified **9**, which largely restored the potency against both rat and human TRPA1 observed for **4**, thus the *p*-Cl-phenyl moiety was selected for further optimization.

A set of compounds was next prepared to examine SAR around the phenyl ring of the quinazolinone core. The poor activity of **10** indicated that the methyl substitution on the phenyl ring was important for the potency of **9**, and data for **11–13** indicated that substitution with a methyl group was

well-tolerated at all but the 7-position of the quinazolinone. Despite the promising potency of these compounds, their microsomal stability remained poor. The relatively good microsomal stability of **10** compared to the methyl-substituted compounds suggested that the methyl groups were likely to be metabolic soft spots. Replacement of the 8-methyl substituent with the trifluoromethyl group in **14** provided a significant improvement with respect to potency but with similarly poor metabolic stability. The fluorinated compound **15** was not as potent as **14** but was significantly more intrinsically stable in both rat and human liver microsomes.

In addition to methyl, trifluoromethyl, and fluoro, the methoxy substituent in **16** also provided a relatively potent inhibitor. On the basis of the apparent potency enhancement provided by either electron-withdrawing or electron-donating substituents, we hypothesized that the quinazolinone core may engage TRPA1 via a π -stacking interaction. Published computational models of the interaction energies of benzene

Table 2. SAR of Oxadiazole Analogues^c


Cmpd	A	B	rTRPA1 IC ₅₀ (μM) ^a	hTRPA1 IC ₅₀ (μM) ^a	RLM/HLM Cl _{int, app} (μL/min/mg)	cLogP
20			0.089	0.156	122 / 35	1.6
21			0.021	0.041	131 / 32	1.6
22			1.40	2.18	52 / 23	0.7
23			0.176	0.136	108 / 38	0.6
24			0.113	0.153	228 / 78	0.6
25			0.314 ^b	0.918 ^b	31 / <14	0.6
26			0.035	0.016	>399 / 340	2.1
27 (AM-0902)			0.024	0.020	41 / <14	0.9
28			0.136	0.211	44 / 19	0.9
29			0.025	0.052 ^b	362 / 84	1.1

^aAntagonist IC₅₀, FLIPR assay. ^bData represents *n* = 1 dose–response curve. ^cData represent the mean of ≥2 independent dose–response curves, except where noted. Standard deviation values are provided in the [Supporting Information](#).

dimers suggest that any substituent enhances π -stacking interaction energy relative to the unsubstituted benzene dimer.¹³ Assuming that the model system predicts the interaction between the substituted benzene ring of an inhibitor and an aromatic residue of the target protein, the relative enhancement of various substituents can be predicted. Indeed, while the precise potency gains over the unsubstituted parent **10** cannot be determined due to its lack of measurable activity, the potencies observed for **9**, **14**, **15**, and **16** align well relative to each other when compared with the predicted values (Figure 2).¹⁴

Increasing polarity is a common strategy for improving the microsomal stability of compounds that are oxidatively metabolized; thus, we sought to decrease the cLogP of the quinazolinones. This strategy was well aligned with further testing of the π -stacking interaction hypothesis, as both nitrile and pyridine substitutions are predicted to have a favorable impact on the π -stacking contribution to potency and would significantly increase polarity. We were pleased to see that nitrile **17** was more potent than earlier compounds, and its cLogP was significantly lower than that of **9–16** (Table 1). As anticipated, the stability of **17** was also improved in rat liver microsomes versus most previously prepared compounds and

the relative stability in human liver microsomes observed for **15** and **16** was maintained. Encouraged by this result, we sought to further reduce cLogP by preparing azaquinazolinones **18** and **19**. Though **18** suffered a decrease in potency relative to **17**, its microsomal stability was promising, as this was the first example of a compound showing very low turnover in both human and rat microsomes. The increased polarity of **18** alone does not account for its improved intrinsic stability. Compound **19**, which has an identical cLogP, was significantly less stable in rat liver microsomes. This suggests that the position of the nitrogen atom in **18** may be key for reducing oxidative metabolism. Notably, the potency data for the nitrile- and pyridine-containing analogues further supports the hypothesis that the core engages TRPA1 through a π -stacking interaction (Figure 2). Though **18** was less potent than HTS hit **4**, its lipophilic efficiency (LipE = 4.3) was improved versus **4** (Figure 3). The azaquinazolinone core was retained for further optimization due to its beneficial effect on microsomal stability, which had been challenging to improve in the parent quinazolinone series.

Having completed initial SAR at both ends of the scaffold, we next turned our attention toward optimization of the amide moiety. A small series of analogues (**20–22**) was prepared that

Table 3. SAR of Analogues Modified To Reduce Metabolism at the Benzylic Position^c

Cmpd	Structure	rTRPA1 IC ₅₀ (μM) ^a	hTRPA1 IC ₅₀ (μM) ^a	RLM / HLM Cl _{int, app} (μL/min/mg)	cLogP
30		1.38 ^b	2.12 ^b	26 / 14	0.2
31		0.075	0.058	19 / <14	0.0
32		0.031	0.041	94 / 56	1.2
33		0.105	0.150	353 / 171	2.0
34		0.652	0.933	14 / 15	2.0
35		0.105	0.116	15 / 25	2.0
36		0.274	0.165	<14 / 76	1.4
37		0.075	0.071	<14 / <14	1.4

^aAntagonist IC₅₀, FLIPR assay. ^bData represents *n* = 1 dose–response curve. ^cData represent the mean of ≥2 independent dose–response curves, except where noted. Standard deviation values are provided in the [Supporting Information](#).

incorporated oxadiazole isomers as replacements for the amide (Table 2). We were pleased to find that the oxadiazoles in **20** and **21** restored or exceeded the potency against both rat and human TRPA1 that had been observed for the most potent quinazolinone amides, with only a relatively small loss of microsomal stability. With cLogP values that are roughly equivalent to amide **18**, the improved potency of compounds **20** and **21** provided significant increases in LipE (5.5 and 6.1, respectively) over **18** (Figure 3). Oxadiazole isomer **22** was not well tolerated. Because the oxadiazole isomer in **21** was approximately 4-fold more potent than isomer **20**, it was selected for further optimization.

Analogues **23–25** were prepared, all of which contain an additional nitrogen atom in the core. None of these compounds showed an improvement in TRPA1 potency and, despite their equivalent increased polarity, only **25** showed an improvement in microsomal stability. A methyl group was also incorporated at the 5-position of the azaquinazolinone core to give compound **26**, as substitution at this position had previously provided a significant improvement in potency. While a moderate potency improvement was observed in human TRPA1 for **26** versus **21**, a significant deterioration in microsomal stability was also observed, which may be expected due to its increase in cLogP and the reintroduction of a likely metabolic soft spot. Similar results were observed on both potency and stability when a methyl group was incorporated at the 2-position of the azaquinazolinone core.¹⁶ Seeking a different approach to

increase polarity, compound **27** (AM-0902) was prepared, which has a low cLogP and also places a methyl group in the space that had repeatedly proven beneficial for TRPA1 activity. Indeed **27** showed good potency against both TRPA1 isoforms, thereby demonstrating a significant improvement in LipE (6.8) versus earlier analogues (Figure 3), and had very good microsomal stability. The observed improvement in potency also supports the π -stacking interaction hypothesis put forward for earlier compounds, as imidazole is predicted to significantly improve a theoretical π -stacking interaction relative to substituted phenyl rings or pyridine (Figure 2).¹⁴ Compound **28**, which contains the alternate oxadiazole isomer, showed a similar decrease in potency that was observed previously between **20** and **21**. The pyrazole isomer **29** had significantly less microsomal stability with similar cLogP, suggesting, in analogy to compounds **18** and **19**, that the specific arrangement of nitrogen atoms in **27** may be critical for reducing oxidative metabolism.

We reasoned that incorporating additional polarity into the phenyl ring might further improve microsomal stability, but polarity was not well tolerated in this region. This trend is exemplified by compound **30** (Table 3). A significant decrease in potency was observed when compared with phenyl analogue **21**, though as anticipated microsomal stability did improve substantially.

Metabolite identification studies in rat and human liver microsomes with **20** and **21** determined that the benzylic

position was the major site of oxidative metabolism. Alcohol **31**, identified as the major metabolite of **21** in microsomes, retained good potency against both rat and human TRPA1 and showed significantly improved microsomal stability (Table 3). Other compounds in which the benzylic position was blocked with less polar substituents, as in **32** and **33**, were relatively potent inhibitors, but the metabolic stability was either comparable to the parent compound (**32** versus **21**) or substantially worse (**33** versus **20**).

Hypothesizing that an olefin may mimic the binding conformation of the saturated analogues while also mitigating oxidative metabolism at the benzylic position, we calculated the lowest energy conformations of the trans-disubstituted and trisubstituted olefins.¹⁵ An overlay with the low energy conformation of the saturated analogue **20** (Figure 4)

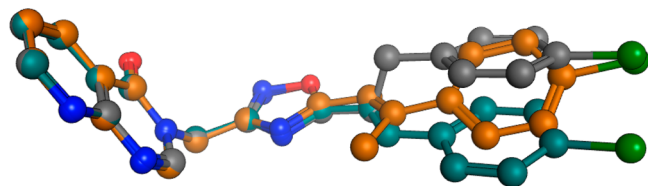


Figure 4. Overlay of the calculated low energy conformations of **20** (gray), **34** (turquoise), and **35** (orange).

suggested that an olefin, and in particular the trisubstituted olefin, may position the critical *p*-chlorophenyl substituent in a similar orientation as the saturated compounds. Indeed, while the potency of **34** was significantly decreased relative to **20**, the trisubstituted olefin **35** restored the potency of the parent compound **20** and improved microsomal stability substantially. The trisubstituted olefin was also well tolerated in the imidazopyrimidinone core, as exemplified by **36** and **37**. Compound **37** was especially noteworthy, as it exhibited sub-100 nM potency against both the rat and human TRPA1 channels with less than detectable turnover in both rat and human liver microsomes. While olefins are typically prone to oxidative metabolism, it is likely that the observed microsomal stability of **34**–**37** is due to the combination of steric hindrance and electron deficiency present in these olefin analogues.

The potencies of compounds of interest were also determined in a radioactive calcium flux assay, which is considered to be a direct measure of TRPA1 potency, as it quantifies only inhibition of $^{45}\text{Ca}^{2+}$ entering the cell upon activation and opening of the channel with AITC. In contrast, the FLIPR assay measures changes in cellular Ca^{2+} levels that can arise from both extracellular and intracellular sources. Data for compounds **4**, **20**, **21**, **27**, **31**, **35**, and **37** show that, despite a right-shift for several of these compounds, the potency observed in the FLIPR assay was generally well maintained in the $^{45}\text{Ca}^{2+}$ flux assay (Table 4).

Protein binding and rat PK data for a subset of analogues are summarized in Table 5. Anticipating that a tool compound used to interrogate the role of TRPA1 in pain would be dosed in acute pain models, we sought to identify a compound that would provide at least 10-fold unbound coverage over its $^{45}\text{Ca}^{2+}$ IC_{50} at maximum concentration (C_{max}) following a moderate dose. A single-dose intravenous (iv) PK experiment showed that compound **21** was cleared at a rate exceeding rat liver blood flow. While also relatively high, compound **20** showed improved iv clearance relative to **21**. As expected for a compound that is both well absorbed and cleared via hepatic

Table 4. Potency of Selected Analogues in the $^{45}\text{Ca}^{2+}$ Flux Assay^a

compd	rTRPA1 IC_{50} (μM) ^b	hTRPA1 IC_{50} (μM) ^b	rTRPA1 EC_{50} (μM) ^c	hTRPA1 EC_{50} (μM) ^c
4	2.62	6.27	>47	>47
20	0.411	1.58	>40	>40
21	0.120	0.376	>40	>40
27	0.071	0.131	>40	>40
31	0.204	0.251	>40	>40
35	0.053	0.085	>40	>40
37	0.055	0.063	>40	>40

^aData represent the mean of ≥ 2 independent dose–response curves.

^bAntagonist IC_{50} , $^{45}\text{Ca}^{2+}$ flux assay. ^cAgonist EC_{50} , $^{45}\text{Ca}^{2+}$ flux assay.

oxidation, **20** also demonstrated moderate oral bioavailability. Despite these improvements, at C_{max} **20** achieved only 3-fold unbound coverage over its $^{45}\text{Ca}^{2+}$ IC_{50} following a 30 mpk oral dose. Compound **27**, while cleared in an iv PK experiment at nearly the same rate as **20**, showed a significantly lower unbound clearance (CL/fu) due to its larger free fraction. While total exposure and oral bioavailability for **20** and **27** were similar, **27** had a higher unbound C_{max} and significantly better potency, which enabled achievement of unbound concentrations that were 31-fold over the $^{45}\text{Ca}^{2+}$ IC_{50} following a 30 mg/kg oral dose. Compound **27** is highly permeable (average $P_{\text{app}} = 44.5 \mu\text{m/s}$ in MDCK cells), an unlikely substrate for P-gp (efflux ratio = 1.3 in P-gp overexpressing MDCK cells), and demonstrates good solubility (PBS pH 7.4: 226 μM , SIF: 248 μM).

The olefins **35** and **37** showed significantly different PK profiles than their saturated analogues. Though low clearance was observed for **35** following iv dosing, its very small free fraction provided an unbound clearance comparable to that of **20**. Consequently, neither **35** nor **37** achieved high multiples over the $^{45}\text{Ca}^{2+}$ IC_{50} following oral dosing, despite their total exposures being much higher and half-lives much longer than that of the saturated analogues.

Additional profiling of compound **27** was performed to assess its selectivity. Compound **27** showed good selectivity over other TRP channels, as no activity was observed against human TRPV1 or TRPV4, or rat TRPV1, TRPV3, or TRPM8, at concentrations up to 10 μM . Activity of **27** was also assessed in a CEREP panel of 40 targets at 10 μM concentration to identify off-target activities, and little to no inhibition was observed (>77 POC against all targets).¹⁶ No activity was detected in CYP 3A4 or CYP2D6 assays (est $\text{IC}_{50} > 27 \mu\text{M}$ for both). Importantly **27** showed only 10% block of Na_v 1.7 channels at 10 μM in mouse DRG neurons, which suggested that any potential efficacy observed in an in vivo pain model would not be due to inhibition of Na_v 1.7.¹⁷

We also measured inhibition of TRPA1 activity induced by agents other than AITC. Compound **27** inhibited $^{45}\text{Ca}^{2+}$ flux upon activation of rat TRPA1 with methylglyoxal, an endogenous and selective agonist,¹⁸ with an IC_{50} of 0.019 μM . Inhibition of $^{45}\text{Ca}^{2+}$ flux was also measured upon activation of rat TRPA1 by changes in osmolarity, which may mimic mechanical activation of the channel,¹⁹ and **27** returned an IC_{50} of 0.010 μM . The potency of compound **27** in these assays showed that its antagonism of TRPA1 was not confined solely to AITC activation and suggested that its activity was likely to extend into physiologically relevant contexts.

Table 5. Protein Binding and Pharmacokinetic Data in Rat for Selected Analogues Following Intravenous and Oral Administration

compd	rat ppb (Fu)	iv ^a					oral ^b					
		CL (L/h/kg)	CL _u	V _{ss} (L/kg)	T _{1/2} (h)	AUC _{inf} (μM·h)	C _{max} (C _{maxu}) (μM)	T _{max} (h)	T _{1/2} (h)	F%	C _{maxu} / ⁴⁵ Ca ²⁺	IC ₅₀
20	0.093	2.2	24	1.0	0.4	19.2	10.3 (1.0)	0.5	4.0	52	3	
21	0.144	5.9	NA ^c	2.0	0.3	ND	ND	ND	ND	ND	—	
27	0.289	2.5	9	1.7	0.6	19.8	7.5 (2.2)	0.8	2.8	60	31	
35	0.012	0.27	22	1.4	4.2	94.9	8.0 (0.1)	2.7	5.1	32	2	
37	0.033	ND	—	ND	ND	117.0	6.5 (0.2)	2.0	10.0	ND	4	

^a0.5 mg/kg, 100% DMSO. ^b30 mg/kg for all except 37 (10 mg/kg), 1% Tween 80/2% HPMC/97% water/methanesulfonic acid pH 2.2. ^cCL_u not calculated, as clearance of high extraction ratio compounds is primarily blood-flow dependent.

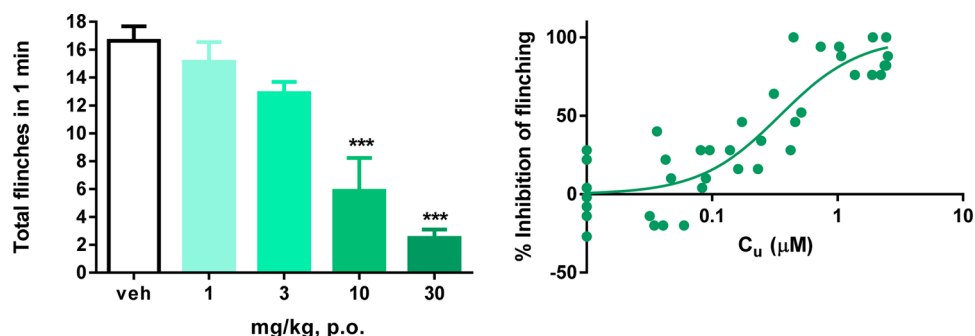
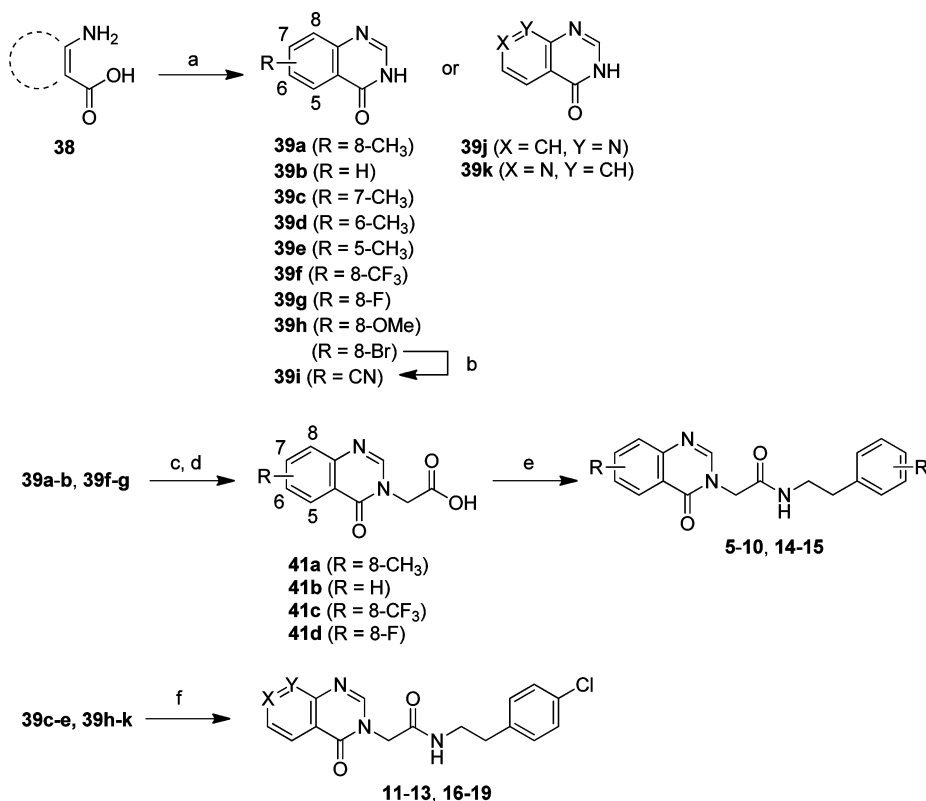


Figure 5. Summary of AITC flinching in rats upon oral administration of 27. (A) Dose-dependent reduction in flinching. (B) Exposure–response relationship. Each point represents an individual animal.

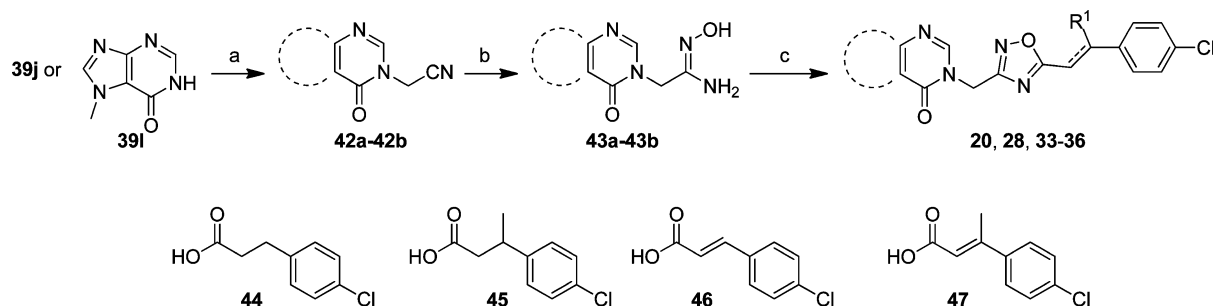
Scheme 1. Synthesis of Amides^a



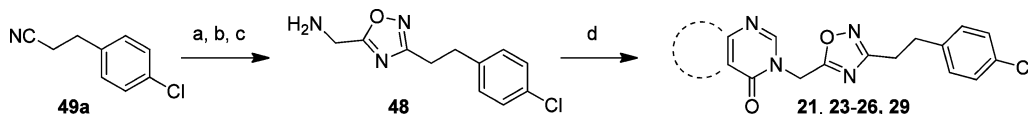
^a**39b** and **39k** were purchased from commercial suppliers. Reagents and conditions: (a) formamide, μW, 175 °C, 1 h; (b) Pd(PPh₃)₄, Zn(CN)₂, DMF, 100 °C; (c) methyl 2-bromoacetate, K₂CO₃, DMF, 50 °C; (d) LiOH, THF/H₂O, RT; (e) T3P, Hünig's base, EtOAc, RT; (f) 2-bromo-N-(4-chlorophenethyl)acetamide (**40**), K₂CO₃, DMF, 50 °C.

The combination of its potent TRPA1 inhibition, oral PK enabling an acceptable projected target coverage, and excellent

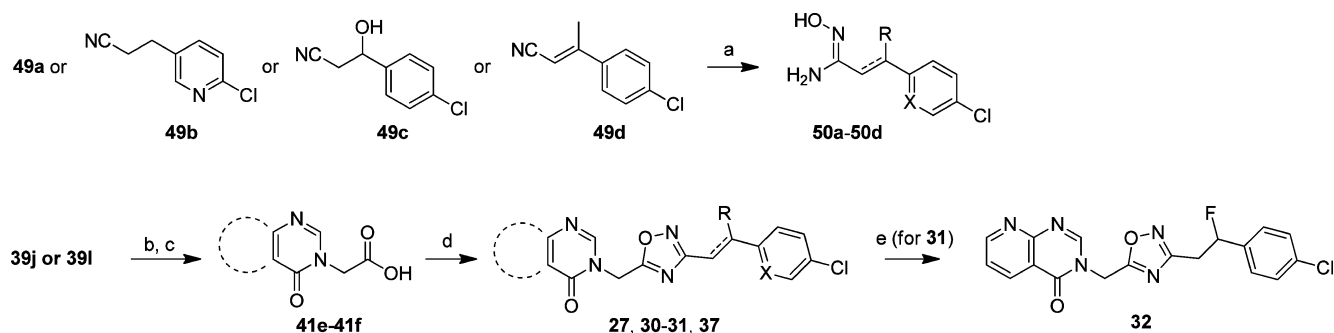
selectivity suggested that compound **27** would be a suitable tool compound to assess the pharmacology of TRPA1 in vivo. To

Scheme 2. Synthesis of Oxadiazoles 20, 28, and 33–36^a

^aReagents and conditions: (a) bromoacetonitrile, K₂CO₃, DMF, 50 °C, 3 h; (b) hydroxylamine, EtOH, 80 °C, 2 h; (c) carboxylic acid **44**, **45**, **46**, or **47**, T3P, Et₃N, EtOAc, 80 °C, 3 h.

Scheme 3. Synthesis of Oxadiazoles 21, 23–26, and 29^a

^aReagents and conditions: (a) hydroxylamine, EtOH, 80 °C, 2 h; (b) *N*-Boc-glycine, Et₃N, T3P, EtOAc, 80 °C, 5 h; (c) TFA, DCM, RT, 17 h; (d) HOBt, EDC-HCl, heteroaryl amino acids, Hünig's Base, DMF, RT, 4 h, then CH(OMe)₃, AcOH, 100 °C, 17 h.

Scheme 4. Synthesis of Oxadiazoles 27, 30–32, and 37^a

^aReagents and conditions: (a) hydroxylamine, EtOH, 80 °C, 2 h; (b) *tert*-butyl bromoacetate, K₂CO₃, DMF, 50 °C, 6 h; (c) concentrated HCl, RT, 30 min; (d) **50**, CDI, DMF, 50–100 °C, 1 h; (e) DAST, DCM, 0 °C to RT, 1 h.

that end, compound **27** was advanced into an *in vivo* model using AITC-induced flinching in rats (Figure 5), which has been reported²⁰ as a useful method for measuring TRPA1 target engagement. Rats were dosed orally with either vehicle (2% HPMC/1% Tween-80) or the TRPA1 antagonist **27** at 1, 3, 10, or 30 mg/kg. After 1 h, one left ventral hind paw was injected with the TRPA1 agonist AITC (0.1%). Nocifensive behavior was then observed and recorded during the first minute postinjection. A dose-dependent reduction of AITC-induced flinching was observed for **27**, with a significant reduction in flinching observed postdosing of 10 and 30 mg/kg. The unbound plasma concentrations (*C_u*) at 1 h for the 1, 3, 10, and 30 mg/kg doses were 0.051 ± 0.024 (*n* = 8), 0.19 ± 0.11 (*n* = 8), 0.58 ± 0.35 (*n* = 8), and 2.2 ± 0.40 (*n* = 8) μ M, covering the *in vitro* rat TRPA1 ⁴⁵Ca²⁺ IC₅₀ at 0.72, 2.7, 8.2, and 30.3 fold, respectively. A good exposure–response relationship was observed in this target coverage model (Figure 5). An unbound *in vivo* IC₅₀ of 0.35 μ M, which is in good agreement with the *in vitro* rat TRPA1 ⁴⁵Ca²⁺ IC₅₀, and unbound *in vivo* IC₉₀ of 1.7 μ M were determined. It is noteworthy that at a dose of 30 mg/kg, **27** engages TRPA1 at concentrations that exceed the *in vivo* IC₉₀, making it a useful tool for exploration of *in vivo* models of acute pain.

CHEMISTRY

Final compounds containing amides were prepared according to the synthesis shown in Scheme 1. Commercially available acids **38** were converted to the corresponding quinazolinone intermediates **39a**, **39c–h**, and **39j** via condensation with formamide. **39i** was prepared via cyanation of the bromide intermediate. Intermediates **39a,b** and **39f,g** were converted to carboxylic acids **41a–d** by regioselective alkylation with methyl 2-bromoacetate followed by saponification with LiOH. T3P-mediated amide coupling then provided final compounds **5–10**, **14**, and **15**. Regioselective alkylation of **39c–e** and **39h–k** with 2-bromo-*N*-(4-chlorophenethyl)acetamide **40** provided compounds **11–13** and **16–19**.

Oxadiazoles **20**, **28**, and **33–37** were prepared according to Scheme 2. Intermediates **39j** and **39l**¹⁶ were converted to nitriles **42a,b** by regioselective alkylation with bromoacetonitrile. Addition of hydroxylamine to the nitriles provided intermediates **43a,b**, which were converted to the oxadiazoles **20**, **28**, and **33–37** via T3P-mediated condensation with carboxylic acids **44–47**.

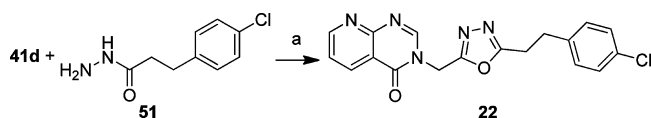
The oxadiazoles **21**, **23–26**, and **29** were prepared according to Scheme 3. Addition of hydroxylamine to 3-(4-chlorophenyl)-

propanenitrile (49a), followed by T3P-mediated condensation with *N*-Boc-glycine and deprotection with TFA, provided the key intermediate 48. Condensation of 48 with commercially available heteroaryl amino acids gave the intermediate amides, which were then condensed with trimethyl orthoformate in acetic acid to provide the final compounds.

The oxadiazoles 27, 30–32, and 37 were prepared using the alternate route detailed in Scheme 4. Intermediates 39j and 39l were converted to the carboxylic acids 41e and 41f via regioselective alkylation with *tert*-butyl bromoacetate followed by removal of the *tert*-butyl group under acidic conditions. The nitrile intermediates 49a–d were treated with hydroxylamine to provide 50a–d. CDI-mediated condensation of 50a–d with either 41d or 41e provided final compounds 27, 30, 31, and 37. Compound 31 was converted to 32 by treatment with DAST.

Oxadiazole 22 was prepared by T3P-mediated condensation of intermediate 41d with 51 (Scheme 5).

Scheme 5. Synthesis of Oxadiazole 22^a



^aReagents and conditions: (a) T3P, Et₃N, EtOAc, 90 °C, 17 h.

CONCLUSIONS

Optimization of high-throughput screening hit 4 led to identification of a potent series of purinone oxadiazole TRPA1 inhibitors. A key strategy for hit optimization was to minimize microsomal turnover by increasing polarity, thereby improving LipE. Design strategy was also informed by a π -stacking hypothesis that may account for the observed potency SAR around the quinazolinone core, and by modeling of low energy conformations, which enabled discovery of the potent and stable trisubstituted olefin analogues. Compound 27 (AM-0902), which is a potent TRPA1 inhibitor across multiple modes of channel activation, is a selective antagonist with pharmacokinetic properties conducive to oral dosing in in vivo target validation studies. Compound 27 showed dose-dependent and nearly complete reduction of AITC-flinching in rats, thereby demonstrating excellent in vivo target coverage. On the basis of published data, 27 may be superior to other known tool compounds reported to date, and disclosure of the efficacy of 27 in in vivo pain models is forthcoming.

EXPERIMENTAL SECTION

Chemistry. Unless otherwise noted, all materials were obtained from commercial suppliers and used without further purification. Compound 4 was purchased from Enamine, and compounds 39b, 39k, 44, 46, and 49a were purchased from common suppliers. Anhydrous solvents were obtained from Aldrich or EM Science and used directly. All microwave-assisted reactions were conducted with Biotage Initiator systems. Silica gel chromatography was performed using prepacked silica gel cartridges and Biotage Isolera One normal phase chromatography systems. Reverse phase chromatography was performed on either a Biotage Isolera Four or Gilson GX-281 system. ¹H NMR spectra were recorded on either a Bruker AVANCE-400 (at 400.13 MHz) or a Bruker AVANCE III-500 (at 500.34 MHz) spectrometer at ambient temperature. Chemical shifts are reported in parts per million (ppm, δ units) relative to residual proton signal in the solvent. Data are reported as follows: chemical shift, multiplicity (s = singlet, d = doublet, t = triplet, q = quartet, br = broad, m = multiplet),

coupling constants (in Hz), and number of protons. Purity for all final compounds was >95% and was measured using one of two Agilent LCMS systems. The first used a HALO C18 from Advanced Materials Technology, 3.0 \times 50 mm, 2.7 μ m column, gradient: 5–95% B over 1.5 min, 1.9 min total run time, 2 mL/min, solvent A: water w/0.1% TFA, solvent B: acetonitrile w/0.1% TFA. The second used a CORTECS C18+ from Waters, 3.0 \times 50 mm, 2.7 μ m column, gradient: 5–95% B over 1.5 min, 2.0 min total run time, 2 mL/min, solvent A: water w/0.1% formic acid, solvent B: acetonitrile w/0.1% formic acid. All final compounds were \geq 95% purity.

All in vivo procedures described in this manuscript were approved by the Institutional Animal Care and Use Committee at Amgen (Thousand Oaks, CA).

General Procedure A: *N*-(4-Chlorophenethyl)-2-(8-methyl-4-oxoquinazolin-3(4H)-yl)acetamide (9). A vial was charged with 2-(8-methyl-4-oxoquinazolin-3(4H)-yl)acetic acid (41a) (75 mg, 0.344 mmol), 2-(4-chlorophenyl)ethanamine (0.064 mL, 0.412 mmol), Hünig's base (0.150 mL, 0.859 mmol), EtOAc (0.678 mL), and 1-propanephosphonic acid cyclic anhydride, 50 wt % solution in EtOAc (0.656 mL, 1.031 mmol), and the mixture was stirred at RT. The mixture became homogeneous initially and then solids crashed out. After 2 h, the solids were filtered and washed with EtOAc to provide the desired compound (43 mg, 35% yield) as an off-white solid. ¹H NMR (400 MHz, DMSO-*d*₆) δ 8.35 (t, *J* = 5.53 Hz, 1 H) 8.28 (s, 1 H) 7.95–8.03 (m, 1 H) 2.55 (s, 3 H) 7.67–7.73 (m, 1 H) 7.43 (t, *J* = 7.63 Hz, 1 H) 7.31–7.37 (m, 2 H) 7.22–7.28 (m, 2 H) 4.54–4.67 (m, 2 H) 3.27–3.34 (m, 2 H) 2.73 (t, *J* = 7.14 Hz, 2 H). MS, *m/z* 356.0 [*M* + *H*]⁺.

General Procedure B: *N*-(4-Chlorophenethyl)-2-(5-methyl-4-oxopyrido[2,3-*d*]pyrimidin-3(4H)-yl)acetamide (13). In a round-bottom flask 5-methylquinazolin-4(3H)-one (39e) (500 mg, 3.12 mmol) was dissolved in 6 mL of DMF. 2-Bromo-*N*-(4-chlorophenethyl)acetamide (40) (1.02 g, 3.74 mmol) and potassium carbonate (646 mg, 4.68 mmol) were added, and the mixture was stirred at 50 °C for 2 h. The mixture was poured into water. The solids were filtered, washed with pentane, and dried over sodium sulfate to provide the title compound as an off-white solid (940 mg, 85% yield). ¹H NMR (400 MHz, DMSO-*d*₆) δ 8.38 (t, *J* = 5.4 Hz, 1 H) 8.22 (s, 1 H) 7.67 (t, *J* = 7.77 Hz, 1 H) 7.50 (d, *J* = 8.0 Hz, 1 H) 7.34 (t, *J* = 7.8 Hz, 2 H) 7.28 (t, *J* = 7.6 Hz, 2 H) 4.55 (s, 2 H) 3.30 (m, 3 H) 2.77 (s, 3 H) 2.73 (d, *J* = 7.1 Hz, 2 H). MS, *m/z* 356.1 [*M* + *H*]⁺.

General Procedure C: 3-((5-(4-Chlorophenethyl)-1,2,4-oxadiazol-3-yl)methyl)pyrido[2,3-*d*]pyrimidin-4(3H)-one (20). A vial was charged with 3-(4-chlorophenyl)propionic acid (44) (60.6 mg, 0.328 mmol), (Z)-*N'*-hydroxy-2-(4-oxopyrido[2,3-*d*]pyrimidin-3(4H)-yl)-acetimidamide (43a) (72 mg, 0.328 mmol), ethyl acetate (1.31 mL), and triethylamine (0.183 mL, 1.314 mmol). 1-propanephosphonic acid cyclic anhydride, 50 wt % solution in ethyl acetate (0.836 mL, 1.314 mmol) was added, and the reaction was heated at 80 °C for 3 h. Water and additional EtOAc were added, and the layers were separated. The organic portion was dried over sodium sulfate, filtered, and concentrated in vacuo. The crude material was purified by silica gel chromatography with a gradient of 0–50% 90/10 DCM/MeOH in DCM to provide the title compound (67 mg, 0.182 mmol, 55.5% yield) as a white solid. ¹H NMR (400 MHz, DMSO-*d*₆) δ ppm 9.02 (dd, *J* = 4.60, 2.05 Hz, 1 H) 8.55 (dd, *J* = 7.92, 1.86 Hz, 1 H) 8.74 (s, 1 H) 7.62 (dd, *J* = 7.92, 4.60 Hz, 1 H) 7.25 (d, *J* = 4.01 Hz, 4 H) 5.37 (s, 2 H) 3.21–3.27 (m, 2 H) 2.98–3.05 (m, 2 H). MS, *m/z* 367.9 [*M* + *H*]⁺.

General Procedure D: 3-((3-(4-Chlorophenethyl)-1,2,4-oxadiazol-5-yl)methyl)pyrido[2,3-*d*]pyrimidin-4(3H)-one (21). A vial was charged with 2-aminonicotinic acid (87 mg, 0.631 mmol), (3-(4-chlorophenethyl)-1,2,4-oxadiazol-5-yl)methanamine (48) (150 mg, 0.631 mmol), HOBt (145 mg, 0.947 mmol), DMF (2524 μ L), and Hünig's base (441 μ L, 2.52 mmol). EDC-HCl (181 mg, 0.947 mmol) was added, and the reaction was stirred at RT for 4 h. Water and EtOAc were added, and the layers were separated. The organic portion was dried over sodium sulfate, filtered, and concentrated. The crude material was slurried in trimethyl orthoformate (1390 μ L, 12.58 mmol) and acetic acid (72.0 μ L, 1.258 mmol), and the mixture was

heated at 100 °C for 17 h. Water and EtOAc were added, and the layers were separated. The organic portion was dried over sodium sulfate, filtered, and concentrated. The crude material was purified by silica gel chromatography, using a gradient of 0–50% 90/10 DCM/MeOH in DCM. The product containing fractions were combined and concentrated. The solids were triturated in diethyl ether, filtered, and air-dried to provide the title compound as an off-white solid (163 mg, 0.443 mmol, 71% yield). ¹H NMR (400 MHz, DMSO-*d*₆) δ 9.03 (dd, *J* = 4.60, 2.05 Hz, 1 H) 8.74–8.77 (m, 1 H) 8.57 (dd, *J* = 7.92, 2.05 Hz, 1 H) 7.59–7.67 (m, 1 H) 7.25–7.31 (m, 2 H) 7.19–7.23 (m, 2 H) 5.56 (s, 2 H) 2.88–3.02 (m, 4 H). MS, *m/z* 368.0 [M + H]⁺.

General Procedure E: 1-((3-(4-Chlorophenethyl)-1,2,4-oxadiazol-5-yl)methyl)-7-methyl-1H-purin-6(7H)-one (27). 2-(7-Methyl-6-oxo-6,7-dihydro-1H-purin-1-yl)acetic acid hydrochloride (**41f**) (0.100 g, 0.409 mmol) was added to a round-bottom flask followed by DMF (1.6 mL) and CDI (0.073 g, 0.450 mmol). The mixture was stirred at 50 °C for 30 min, (Z)-3-(4-chlorophenyl)-*N*'-hydroxypropanimide (**50a**) (0.81 g, 0.409 mmol) was added, and the temperature was increased to 100 °C. After 1 h, the mixture was cooled to room temperature, water and DCM were added, and the layers were separated. The aqueous portion was extracted with additional DCM, and the combined organic portions were dried over sodium sulfate, filtered, and concentrated. The crude material was purified by silica gel chromatography, 0–50% 90/10 DCM/MeOH in DCM to provide the title compound (0.044 g, 24% yield) as a white solid. ¹H NMR (400 MHz, DMSO-*d*₆) δ ppm 8.45 (s, 1 H), 8.24 (s, 1 H), 7.26–7.31 (m, 2 H), 7.21–7.26 (m, 2 H), 5.53 (s, 2 H), 3.95 (s, 3 H), 2.88–3.02 (m, 4 H). MS, *m/z* 371.0 [M + H]⁺.

General Procedure F: 7-Methylquinazolin-4(3H)-one (39c). In a 20 mL microwave vial, 2-amino-4-methylbenzoic acid (3.0 g, 19.8 mmol) was dissolved in formamide (7.89 mL, 198 mmol). The mixture was irradiated at 150 °C for 1 h in the microwave. The mixture was diluted with water, and the resulting solids were filtered, rinsed with water, and air-dried to yield the title compound (2.0 g, 63% yield) as an off-white solid. ¹H NMR (400 MHz, DMSO-*d*₆) δ 12.16 (br s, 1H), 8.05 (s, 1H), 8.00 (d, *J* = 8.4, 1H), 7.48 (s, 1H), 7.34 (d, *J* = 8.0, 1H), 2.46 (s, 3H). MS, *m/z* 161.3 [M + H]⁺.

2-(8-Methyl-4-oxoquinazolin-3(4H)-yl)-*N*-phenethylacetamide (5). The title compound was prepared according to general procedure A using 2-(8-methyl-4-oxoquinazolin-3(4H)-yl)acetic acid (**41a**) and 2-phenylethanamine as a white solid in 70% yield. ¹H NMR (400 MHz, DMSO-*d*₆) δ ppm 8.42–8.49 (m, 1 H), 8.37 (s, 1 H), 8.02–8.09 (m, 1 H), 7.74–7.80 (m, 1 H), 7.47–7.54 (m, 1 H), 7.34–7.40 (m, 2 H), 7.32 (s, 3 H), 4.70 (s, 2 H), 3.34–3.43 (m, 2 H), 2.76–2.85 (m, 2 H), 2.63 (s, 3 H). MS, *m/z* 322.0 [M + H]⁺.

***N*-(4-Methoxyphenethyl)-2-(8-methyl-4-oxoquinazolin-3(4H)-yl)-acetamide (6).** The title compound was prepared according to general procedure A using 2-(8-methyl-4-oxoquinazolin-3(4H)-yl)acetic acid (**41a**) and 2-(4-methoxyphenyl)ethanamine as a white solid in 52% yield. ¹H NMR (400 MHz, DMSO-*d*₆) δ ppm 8.31–8.37 (m, 1 H), 8.29 (s, 1 H), 7.95–8.01 (m, 1 H), 7.66–7.72 (m, 1 H), 7.39–7.46 (m, 1 H), 7.10–7.17 (m, 2 H), 6.79–6.88 (m, 2 H), 4.62 (s, 2 H), 3.72 (s, 3 H), 3.23–3.30 (m, 2 H), 2.63–2.71 (m, 2 H), 2.53–2.57 (m, 3 H). MS, *m/z* 352.0 [M + H]⁺.

***N*-(3-Methoxyphenethyl)-2-(8-methyl-4-oxoquinazolin-3(4H)-yl)-acetamide (7).** The title compound was prepared according to general procedure A using 2-(8-methyl-4-oxoquinazolin-3(4H)-yl)acetic acid (**41a**) and 2-(3-methoxyphenyl)ethanamine as a white solid in 65% yield. ¹H NMR (400 MHz, DMSO-*d*₆) δ ppm 8.34–8.39 (m, 1 H), 8.29 (s, 1 H), 7.95–8.00 (m, 1 H), 7.67–7.72 (m, 1 H), 7.38–7.47 (m, 1 H), 7.14–7.23 (m, 1 H), 6.74–6.82 (m, 3 H), 4.59–4.64 (m, 2 H), 3.75 (s, 3 H), 3.28–3.35 (m, 2 H), 2.68–2.74 (m, 2 H), 2.54–2.58 (m, 3 H). MS, *m/z* 352.0 [M + H]⁺.

***N*-(2-Methoxyphenethyl)-2-(8-methyl-4-oxoquinazolin-3(4H)-yl)-acetamide (8).** The title compound was prepared according to general procedure A using 2-(8-methyl-4-oxoquinazolin-3(4H)-yl)acetic acid (**41a**) and 2-(2-methoxyphenyl)ethanamine as a white solid in 75% yield. ¹H NMR (400 MHz, DMSO-*d*₆) δ ppm 8.32–8.38 (m, 1 H), 8.28 (s, 1 H), 7.94–8.01 (m, 1 H), 7.67–7.72 (m, 1 H), 7.40–7.46 (m, 1 H), 7.17–7.24 (m, 1 H), 7.11–7.16 (m, 1 H), 6.93–6.98 (m, 1

H), 6.83–6.91 (m, 1 H), 4.62 (s, 2 H), 3.79 (s, 3 H), 3.23–3.31 (m, 2 H), 2.69–2.76 (m, 2 H), 2.55 (s, 3 H). MS, *m/z* 352.0 [M + H]⁺.

***N*-(4-Chlorophenethyl)-2-(4-oxoquinazolin-3(4H)-yl)-acetamide (10).** The title compound was prepared according to general procedure A using 2-(4-oxoquinazolin-3(4H)-yl)acetic acid (**41b**) and 2-(4-chlorophenyl)ethanamine as a white solid in 40% yield. ¹H NMR (400 MHz, DMSO-*d*₆) δ ppm 8.33–8.38 (m, 1 H), 8.24–8.28 (m, 1 H), 8.12–8.16 (m, 1 H), 7.81–7.87 (m, 1 H), 7.67–7.72 (m, 1 H), 7.52–7.58 (m, 1 H), 7.31–7.36 (m, 2 H), 7.23–7.28 (m, 2 H), 4.58–4.63 (m, 2 H), 4.58–4.63 (m, 2 H), 2.70–2.75 (m, 2 H). MS, *m/z* 342.0 [M + H]⁺.

***N*-(4-Chlorophenethyl)-2-(7-methyl-4-oxoquinazolin-3(4H)-yl)-acetamide (11).** The title compound was prepared according to general procedure B using 7-methylquinazolin-4(3H)-one (**39c**) and 2-bromo-*N*-(4-chlorophenethyl)acetamide (**40**) as a yellow solid in 85% yield. ¹H NMR (400 MHz, DMSO-*d*₆) δ 8.43 (s, 1H), 8.28 (s, 1H), 8.00 (d, *J* = 8.4, 1H), 7.54 (s, 1H), 7.43–7.37 (m, 3H), 7.31 (d, *J* = 8.4, 2H), 4.63 (s, 2H), 3.39–3.31 (m, 2H), 2.76 (t, *J* = 7.2, 2H), 2.51 (s, 3H). MS, *m/z* 355.8 [M + H]⁺.

***N*-(4-Chlorophenethyl)-2-(6-methyl-4-oxoquinazolin-3(4H)-yl)-acetamide (12).** The title compound was prepared according to general procedure B using 6-methylquinazolin-4(3H)-one (**39d**) and 2-bromo-*N*-(4-chlorophenethyl)acetamide (**40**) as a yellow solid in 80% yield. ¹H NMR (400 MHz, DMSO-*d*₆) δ 8.38 (s, 1H), 8.21 (s, 1H), 7.94 (s, 1H), 7.68–7.58 (m, 2H), 7.35–7.24 (m, 4H), 4.60 (s, 2H), 3.34–3.29 (m, 2H), 2.74–2.72 (m, 2H), 2.45 (s, 3H). MS, *m/z* 355.9 [M + H]⁺.

***N*-(4-Chlorophenethyl)-2-(4-oxo-8-(trifluoromethyl)quinazolin-3(4H)-yl)acetamide (14).** The title compound was prepared according to general procedure A using 2-(4-oxo-8-(trifluoromethyl)quinazolin-3(4H)-yl)acetic acid (**41c**) and 2-(4-chlorophenyl)ethanamine as an off-white solid in 31% yield. ¹H NMR (400 MHz, DMSO-*d*₆) δ 8.43 (s, 1 H), 8.37–8.45 (m, 2 H), 8.23 (dd, *J* = 7.53, 0.88 Hz, 1 H), 7.70 (t, *J* = 7.73 Hz, 1 H), 7.31–7.36 (m, 2 H), 7.24–7.28 (m, 2 H), 4.65 (s, 2 H), 3.30–3.36 (m, 2 H), 2.69–2.77 (m, 2 H). MS, *m/z* 410.0 [M + H]⁺.

***N*-(4-Chlorophenethyl)-2-(8-fluoro-4-oxoquinazolin-3(4H)-yl)-acetamide (15).** The title compound was prepared according to general procedure A using 2-(8-fluoro-4-oxoquinazolin-3(4H)-yl)acetic acid (**41d**) and 2-(4-chlorophenyl)ethanamine as an off-white solid in 43% yield. ¹H NMR (400 MHz, DMSO-*d*₆) δ ppm 8.34–8.41 (m, 1 H), 8.33 (s, 1 H), 7.93–7.98 (m, 1 H), 7.68–7.76 (m, 1 H), 7.51–7.58 (m, 1 H), 7.31–7.37 (m, 2 H), 7.22–7.28 (m, 2 H), 4.63 (s, 2 H), 3.30–3.35 (m, 2 H), 2.69–2.76 (m, 2 H). MS, *m/z* 360.0 [M + H]⁺.

***N*-(4-Chlorophenethyl)-2-(8-methoxy-4-oxoquinazolin-3(4H)-yl)-acetamide (16).** The title compound was prepared according to general procedure B using 8-methoxyquinazolin-4(3H)-one (**39h**) and 2-bromo-*N*-(4-chlorophenethyl)acetamide (**40**) as a yellow solid in 6% yield. ¹H NMR (500 MHz, DMSO-*d*₆) δ ppm 8.35 (t, *J* = 5.50 Hz, 1 H), 8.21 (s, 1 H), 7.68 (d, *J* = 8.01 Hz, 1 H), 7.48 (t, *J* = 7.96 Hz, 1 H), 7.32–7.40 (m, 3 H), 7.26 (d, *J* = 7.85 Hz, 2 H), 4.61 (s, 2 H), 3.92 (s, 3 H), 3.31 (s, 4 H), 2.72 (t, *J* = 7.21 Hz, 2 H), 2.50 (br s, 6 H), 0.04 (s, 1 H). MS, *m/z* 372.0 [M + H]⁺.

***N*-(4-Chlorophenethyl)-2-(8-cyano-4-oxoquinazolin-3(4H)-yl)-acetamide (17).** The title compound was prepared according to general procedure B using 4-oxo-3,4-dihydroquinazoline-8-carbonitrile (**39i**) and 2-bromo-*N*-(4-chlorophenethyl)acetamide (**40**) as a white solid in 72% yield. ¹H NMR (400 MHz, DMSO-*d*₆) δ 8.49 (s, 1 H) 8.34–8.44 (m, 3 H) 7.70 (t, *J* = 7.78 Hz, 1 H) 7.31–7.37 (m, 2 H) 7.23–7.29 (m, 2 H) 4.65 (s, 2 H) 3.30–3.36 (m, 2 H) 2.73 (t, *J* = 7.14 Hz, 2 H). MS, *m/z* 366.8 [M + H]⁺.

***N*-(4-Chlorophenethyl)-2-(4-oxopyrido[2,3-*d*]pyrimidin-3(4H)-yl)-acetamide (18).** The title compound was prepared according to general procedure B using pyrido[2,3-*d*]pyrimidin-4(3H)-one (**39j**) and 2-bromo-*N*-(4-chlorophenethyl)acetamide (**40**) as a yellow solid in 64% yield. ¹H NMR (400 MHz, DMSO-*d*₆) δ 8.99 (dd, *J* = 4.55, 2.01 Hz, 1 H) 8.55 (dd, *J* = 7.92, 1.96 Hz, 1 H) 8.47–8.51 (m, 1 H) 8.40 (t, *J* = 5.67 Hz, 1 H) 7.59 (dd, *J* = 7.87, 4.55 Hz, 1 H) 7.31–7.38 (m, 2 H) 7.23–7.28 (m, 2 H) 4.64 (s, 2 H) 3.27–3.34 (m, 2 H) 2.69–2.75 (m, 2 H). MS, *m/z* 342.8 [M + H]⁺.

N-(4-Chlorophenethyl)-2-(4-oxopyrido[3,4-*d*]pyrimidin-3(4*H*)-yl)-acetamide (**19**). The title compound was prepared according to general procedure B using pyrido[3,4-*d*]pyrimidin-4(3*H*)-one (**39k**) and 2-bromo-*N*-(4-chlorophenethyl)acetamide (**40**) as an off-white solid in 14% yield. ¹H NMR (400 MHz, DMSO-*d*₆) δ ppm 9.08–9.12 (m, 1 H), 8.68–8.73 (m, 1 H), 8.41–8.43 (m, 1 H), 8.34–8.41 (m, 1 H), 7.97–8.01 (m, 1 H), 7.31–7.36 (m, 2 H), 7.21–7.29 (m, 2 H), 4.60–4.67 (m, 2 H), 3.30–3.35 (m, 2 H), 2.69–2.76 (m, 2 H). MS, *m/z* 343.2 [M + H]⁺.

3-((5-(4-Chlorophenethyl)-1,3,4-oxadiazol-2-yl)methyl)pyrido[2,3-*d*]pyrimidin-4(3*H*)-one (**22**). A vial was charged with 2-(4-oxopyrido[2,3-*d*]pyrimidin-3(4*H*)-yl)acetic acid (**41d**) (80 mg, 0.390 mmol), 3-(4-chlorophenyl)propanehydrazide (**51**) (93 mg, 0.468 mmol), EtOAc (0.260 mL), DMF (0.520 mL), and triethylamine (0.163 mL, 1.170 mmol). 1-Propanephosphonic acid cyclic anhydride, 50 wt % solution in ethyl acetate (0.744 mL, 1.170 mmol), was added, and the mixture was stirred overnight at 90 °C. Water and EtOAc were added, and the layers were separated. The organic portion was dried over sodium sulfate, filtered, and concentrated. The crude material was purified by silica gel chromatography, using a gradient of 0–50% 90/10 DCM/MeOH in DCM to provide the desired compound (25 mg, 0.068 mmol, 18% yield) as an off white solid. ¹H NMR (400 MHz, DMSO-*d*₆) δ 9.02 (dd, *J* = 2.01, 4.55 Hz, 1H), 8.69–8.76 (m, 1H), 8.52–8.60 (m, 1H), 7.57–7.68 (m, 1H), 7.21–7.30 (m, 4H), 5.48 (s, 2H), 3.12–3.22 (m, 2H), 2.95–3.04 (m, 2H). MS, *m/z* 367.9 [M + H]⁺.

6-((3-(4-Chlorophenethyl)-1,2,4-oxadiazol-5-yl)methyl)pyrimido[4,5-*c*]pyridazin-5(6*H*)-one (**23**). The title compound was prepared according to general procedure D using 3-aminopyridazine-4-carboxylic acid and (3-(4-chlorophenethyl)-1,2,4-oxadiazol-5-yl)-methanamine (**48**) as an off-white solid in 25% yield. ¹H NMR (400 MHz, DMSO-*d*₆) δ 9.58 (d, *J* = 5.18 Hz, 1 H) 8.83–8.91 (m, 1 H) 8.35 (d, *J* = 5.18 Hz, 1 H) 7.25–7.32 (m, 2 H) 7.18–7.24 (m, 2 H) 5.52–5.62 (m, 2 H) 2.86–3.03 (m, 4 H). MS, *m/z* 368.8 [M + H]⁺.

3-((3-(4-Chlorophenethyl)-1,2,4-oxadiazol-5-yl)methyl)pyrimido[4,5-*d*]pyrimidin-4(3*H*)-one (**24**). The title compound was prepared according to general procedure D using 4-aminopyrimidine-5-carboxylic acid and (3-(4-chlorophenethyl)-1,2,4-oxadiazol-5-yl)-methanamine (**48**) as a white solid in 51% yield. ¹H NMR (400 MHz, DMSO-*d*₆) δ 9.56 (s, 1 H) 9.50 (s, 1 H) 8.97 (s, 1 H) 7.25–7.35 (m, 2 H) 7.18–7.24 (m, 2 H) 5.58 (s, 2 H) 2.85–3.06 (m, 4 H). MS, *m/z* 368.8 [M + H]⁺.

3-((3-(4-Chlorophenethyl)-1,2,4-oxadiazol-5-yl)methyl)pteridin-4(3*H*)-one (**25**). The title compound was prepared according to general procedure D using 3-amino-2-pyrazinecarboxylic acid and (3-(4-chlorophenethyl)-1,2,4-oxadiazol-5-yl)methanamine (**48**) as a light yellow solid in 70% yield. ¹H NMR (400 MHz, DMSO-*d*₆) δ 9.07–9.11 (m, 1 H) 8.92–8.96 (m, 1 H) 8.84 (s, 1 H) 7.25–7.30 (m, 2 H) 7.18–7.25 (m, 2 H) 5.60 (s, 2 H) 2.96–3.03 (m, 2 H) 2.90–2.96 (m, 2 H). MS, *m/z* 369.0 [M + H]⁺.

3-((3-(4-Chlorophenethyl)-1,2,4-oxadiazol-5-yl)methyl)-5-methylpyrido[2,3-*d*]pyrimidin-4(3*H*)-one (**26**). The title compound was prepared according to general procedure D using 2-amino-4-methylnicotinic acid and (3-(4-chlorophenethyl)-1,2,4-oxadiazol-5-yl)methanamine (**48**) as an off-white solid in 20% yield. ¹H NMR (400 MHz, DMSO-*d*₆) δ 8.79 (d, *J* = 4.79 Hz, 1 H) 8.68–8.72 (m, 1 H) 7.41 (dd, *J* = 4.84, 0.83 Hz, 1 H) 7.24–7.29 (m, 2 H) 7.19–7.24 (m, 2 H) 5.50 (s, 2 H) 2.89–3.03 (m, 4 H) 2.76 (s, 3 H). MS, *m/z* 381.9 [M + H]⁺.

1-((5-(4-Chlorophenethyl)-1,2,4-oxadiazol-3-yl)methyl)-7-methyl-1*H*-purin-6(7*H*)-one (**28**). The title compound was prepared according to general procedure C using 3-(4-chlorophenyl)propionic acid (**44**) and (Z)-*N'*-hydroxy-2-(7-methyl-6-oxo-6,7-dihydro-1*H*-purin-1-yl)acetimidamide (**43b**) as an off-white solid in 32% yield. ¹H NMR (400 MHz, DMSO-*d*₆) δ 8.39–8.44 (m, 1H), 8.19–8.24 (m, 1H), 7.22–7.30 (m, 4H), 5.31–5.40 (m, 2H), 3.95 (s, 3H), 3.18–3.28 (m, 2H), 2.97–3.05 (m, 2H). MS, *m/z* 371.0 [M + H]⁺.

6-((3-(4-Chlorophenethyl)-1,2,4-oxadiazol-5-yl)methyl)-1-methyl-1*H*-pyrazolo[4,3-*d*]pyrimidin-7(6*H*)-one (**29**). The title compound was prepared according general procedure D using 4-amino-2-methyl-2*H*-pyrazole-3-carboxylic acid and (3-(4-chlorophenethyl)-1,2,4-oxa-

diazol-5-yl)methanamine (**48**) as a white solid in 15% yield. ¹H NMR (400 MHz, DMSO-*d*₆) δ 8.30–8.35 (m, 1 H) 8.05–8.08 (m, 1 H) 7.25–7.30 (m, 2 H) 7.20–7.25 (m, 2 H) 5.55 (s, 2 H) 4.19 (s, 3 H) 2.96–3.02 (m, 2 H) 2.90–2.96 (m, 2 H). MS, *m/z* 371.0 [M + H]⁺.

3-((3-(2-(6-Chloropyridin-3-yl)ethyl)-1,2,4-oxadiazol-5-yl)-methyl)pyrido[2,3-*d*]pyrimidin-4(3*H*)-one (**30**). The title compound was prepared according to general procedure E using 2-(4-oxopyrido[2,3-*d*]pyrimidin-3(4*H*)-yl)acetic acid hydrochloride (**41e**) and (Z)-3-(6-chloropyridin-3-yl)-*N'*-hydroxypropanimidamide (**50b**) as a yellow solid in 85% yield. ¹H NMR (400 MHz, DMSO-*d*₆) δ 9.03 (dd, *J* = 1.96, 4.60 Hz, 1H), 8.76 (s, 1H), 8.57 (dd, *J* = 2.05, 7.92 Hz, 1H), 8.20–8.30 (m, 1H), 7.71 (dd, *J* = 2.54, 8.22 Hz, 1H), 7.63 (dd, *J* = 4.55, 7.97 Hz, 1H), 7.37 (d, *J* = 8.22 Hz, 1H), 5.51–5.62 (m, 2H), 2.92–3.07 (m, 4H). MS, *m/z* 369.0 [M + H]⁺.

3-((3-(2-(4-Chlorophenyl)-2-hydroxyethyl)-1,2,4-oxadiazol-5-yl)-methyl)pyrido[2,3-*d*]pyrimidin-4(3*H*)-one (**31**). The title compound was prepared according to general procedure E using 2-(4-oxopyrido[2,3-*d*]pyrimidin-3(4*H*)-yl)acetic acid hydrochloride (**41e**) and (Z)-3-(4-chlorophenyl)-*N'*,3-dihydroxypropanimidamide (**50c**) as an off-white solid in 23% yield. ¹H NMR (400 MHz, DMSO-*d*₆) δ 9.04 (dd, *J* = 2.05, 4.60 Hz, 1H), 8.76 (s, 1H), 8.58 (dd, *J* = 2.05, 7.92 Hz, 1H), 7.60–7.67 (m, 1H), 7.28–7.37 (m, 4H), 5.60 (d, *J* = 4.79 Hz, 1H), 5.56 (s, 2H), 4.92 (td, *J* = 5.39, 7.70 Hz, 1H), 2.94–3.01 (m, 2H). MS, *m/z* 384.0 [M + H]⁺.

3-((3-(2-(4-Chlorophenyl)-2-fluoroethyl)-1,2,4-oxadiazol-5-yl)-methyl)pyrido[2,3-*d*]pyrimidin-4(3*H*)-one (**32**). In a sealed tube, 3-((3-(2-(4-chlorophenyl)-2-hydroxyethyl)-1,2,4-oxadiazol-5-yl)-methyl)pyrido[2,3-*d*]pyrimidin-4(3*H*)-one (**31**) (0.012 mg, 0.031 mmol) was dissolved in DCM (0.063 mL). The solution was cooled to 0 °C, and (diethylamino)sulfur trifluoride (0.012 mL, 0.094 mmol) was added dropwise. The mixture was allowed to warm to RT and stirred for 1 h. The reaction was carefully quenched with sodium bicarbonate and was extracted into DCM. The organic portion was washed with water and brine, dried with sodium sulfate, filtered through a fritted funnel, and concentrated. The crude product was purified with silica gel chromatography using a gradient of 25–70% DCM:MeOH(90:10)/DCM to provide the desired compound as a racemic mixture (7 mg, 0.018 mmol, 58.0% yield) as a tan solid. ¹H NMR (400 MHz, DMSO-*d*₆) δ 9.04 (dd, *J* = 1.96, 4.60 Hz, 1H), 8.77 (s, 1H), 8.57 (dd, *J* = 2.05, 7.92 Hz, 1H), 7.61–7.66 (m, 1H), 7.39–7.51 (m, 5H), 5.84–6.03 (m, 1H), 5.59 (s, 2H), 3.41–3.53 (m, 1H), 3.34–3.41 (m, 1H). MS, *m/z* 386.0 [M + H]⁺.

3-((5-(2-(4-Chlorophenyl)propyl)-1,2,4-oxadiazol-3-yl)methyl)pyrido[2,3-*d*]pyrimidin-4(3*H*)-one (**33**). The title compound was prepared according to general procedure C using 3-(4-chlorophenyl)-butanoic acid (**45**) and (Z)-*N'*-hydroxy-2-(4-oxopyrido[2,3-*d*]pyrimidin-3(4*H*)-yl)acetimidamide (**43a**) as an off-white solid in 26% yield. ¹H NMR (400 MHz, DMSO-*d*₆) δ 9.02 (dd, *J* = 2.05, 4.60 Hz, 1H), 8.71 (s, 1H), 8.54 (dd, *J* = 2.01, 7.87 Hz, 1H), 7.62 (dd, *J* = 4.55, 7.97 Hz, 1H), 7.25 (s, 4H), 5.34 (s, 2H), 3.20–3.30 (m, 3H), 1.23 (d, *J* = 6.55 Hz, 3H). MS, *m/z* 382.0 [M + H]⁺.

(*E*)-3-((5-(4-Chlorostyryl)-1,2,4-oxadiazol-3-yl)methyl)pyrido[2,3-*d*]pyrimidin-4(3*H*)-one (**34**). The title compound was prepared according to general procedure C using (*E*)-3-(4-chlorophenyl)acrylic acid (**46**) and (Z)-*N'*-hydroxy-2-(4-oxopyrido[2,3-*d*]pyrimidin-3(4*H*)-yl)acetimidamide (**43a**) as an off-white solid in 43% yield. ¹H NMR (400 MHz, DMSO-*d*₆) δ 8.99–9.05 (m, 1H), 8.75–8.82 (m, 1H), 8.52–8.59 (m, 1H), 7.85–7.89 (m, 1H), 7.82–7.86 (m, 2H), 7.62 (dd, *J* = 4.60, 7.92 Hz, 1H), 7.48–7.54 (m, 2H), 7.41 (d, *J* = 16.53 Hz, 1H), 5.45 (s, 2H). MS, *m/z* 366.0 [M + H]⁺.

(*E*)-3-((5-(2-(4-Chlorophenyl)prop-1-en-1-yl)-1,2,4-oxadiazol-3-yl)methyl)pyrido[2,3-*d*]pyrimidin-4(3*H*)-one (**35**). The title compound was prepared according to general procedure C using (*E*)-3-(4-chlorophenyl)but-2-enoic acid (**47**) and (Z)-*N'*-hydroxy-2-(4-oxopyrido[2,3-*d*]pyrimidin-3(4*H*)-yl)acetimidamide (**43a**) as an off-white solid in 42% yield. ¹H NMR (400 MHz, DMSO-*d*₆) δ 9.00–9.05 (m, 1H), 8.77–8.83 (m, 1H), 8.54–8.59 (m, 1H), 7.69–7.77 (m, 2H), 7.58–7.66 (m, 1H), 7.45–7.54 (m, 2H), 6.91–6.96 (m, 1H), 5.47 (s, 2H), 2.60 (d, *J* = 1.27 Hz, 3H). MS, *m/z* 380.0 [M + H]⁺.

(*E*)-1-((5-(2-(4-Chlorophenyl)prop-1-en-1-yl)-1,2,4-oxadiazol-3-yl)methyl)-7-methyl-1H-purin-6(7H)-one (**36**). The title compound was prepared according to general procedure c using (*E*)-3-(4-chlorophenyl)but-2-enoic acid (**47**) and (*Z*)-*N'*-hydroxy-2-(7-methyl-6-oxo-6,7-dihydro-1H-purin-1-yl)acetimidamide (**43b**) as a white solid in 42% yield. ¹H NMR (400 MHz, DMSO-*d*₆) δ 8.48 (s, 1H), 8.22 (s, 1H), 7.74 (d, *J* = 8.61 Hz, 2H), 7.51 (d, *J* = 8.71 Hz, 2H), 6.94 (d, *J* = 0.98 Hz, 1H), 5.45 (s, 2H), 3.96 (s, 3H), 2.61 (s, 3H). MS, *m/z* 383.0 [M + H]⁺.

(*E*)-1-((3-(2-(4-Chlorophenyl)prop-1-en-1-yl)-1,2,4-oxadiazol-5-yl)methyl)-7-methyl-1H-purin-6(7H)-one (**37**). The title compound was prepared according to general procedure E using 2-(7-methyl-6-oxo-6,7-dihydro-1H-purin-1-yl)acetic acid hydrochloride (**41f**) and (1*Z*,2*E*)-3-(4-chlorophenyl)-*N'*-hydroxybut-2-enimidamide (**50d**) as an off-white solid in 45% yield. ¹H NMR (400 MHz, DMSO-*d*₆) δ 8.49 (s, 1H), 8.25 (s, 1H), 7.65–7.68 (m, 2H), 7.45–7.49 (m, 2H), 6.70 (d, *J* = 1.27 Hz, 1H), 5.61 (s, 2H), 3.96 (s, 3H), 3.32 (s, 3H). MS, *m/z* 383.1 [M + H]⁺.

8-Methylquinazolin-4(3H)-one (**39a**). The title compound was prepared according to general procedure F using 2-amino-3-methylbenzoic acid as an off-white solid in 29% yield. ¹H NMR (400 MHz, DMSO-*d*₆) δ 12.19 (br s, 1H), 8.10 (s, 1H), 7.96 (dd, *J* = 0.98, 7.92 Hz, 1H), 7.64–7.70 (m, 1H), 7.36–7.43 (m, 1H), 2.52–2.56 (m, 3H). MS, *m/z* 161.2 [M + H]⁺.

6-Methylquinazolin-4(3H)-one (**39d**). The title compound was prepared according to general procedure F using 2-amino-5-methylbenzoic acid as a tan solid in 57% yield. ¹H NMR (400 MHz, DMSO-*d*₆) δ 12.16 (s, 1H), 8.05–8.00 (m, 1H), 7.91 (s, 1H), 7.67–7.53 (m, 2H), 2.44 (s, 3H). MS, *m/z* 161.0 [M + H]⁺.

5-Methylquinazolin-4(3H)-one (**39e**). The title compound was prepared according to general procedure F using 2-amino-6-methylbenzoic acid as a white solid in 44% yield. ¹H NMR (400 MHz, DMSO-*d*₆) δ 11.99 (br s, 1H), 7.98 (s, 1H), 7.62 (t, *J* = 7.57 Hz, 1H), 7.46 (d, *J* = 7.73 Hz, 1H), 7.25 (d, *J* = 7.34 Hz, 1H), 2.77 (s, 3H). MS, *m/z* 161.0 [M + H]⁺.

8-(Trifluoromethyl)quinazolin-4(3H)-one (**39f**). The title compound was prepared according to general procedure F using 2-amino-3-(trifluoromethyl)benzoic acid. Water and EtOAc were added, and the layers were separated. The organic portion was dried over sodium sulfate, filtered, and concentrated. The crude material was purified by silica gel chromatography, 0–100% EtOAc/heptane to provide the desired compound in 26% yield as a yellow solid. MS, *m/z* 215.0 [M + H]⁺.

8-Fluoroquinazolin-4(3H)-one (**39g**). The title compound was prepared according to general procedure F using 2-amino-3-fluorobenzoic acid as a tan solid in 57% yield. ¹H NMR (400 MHz, DMSO-*d*₆) δ ppm 12.27–12.52 (m, 1 H), 8.14 (s, 1 H), 7.93 (dt, *J* = 8.00, 1.04 Hz, 1 H), 7.68 (ddd, *J* = 10.66, 8.02, 1.37 Hz, 1 H), 7.51 (td, *J* = 8.02, 4.79 Hz, 1 H). MS, *m/z* 165.0 [M + H]⁺.

8-Methoxyquinazolin-4(3H)-one (**39h**). The title compound was prepared according to general procedure F using 2-amino-3-methoxybenzoic acid as a tan solid in 77% yield. MS, *m/z* 177.0 [M + H]⁺.

4-Oxo-3,4-dihydroquinazoline-8-carbonitrile (**39i**). 8-Bromoquinazolin-4(3H)-one was prepared according to general procedure F using 2-amino-3-bromobenzoic acid as a yellow solid in 54% yield. ¹H NMR (400 MHz, DMSO-*d*₆) δ 12.48 (br s, 1H), 8.21 (s, 1H), 8.08–8.17 (m, 2H), 7.39–7.47 (m, 1H). MS, *m/z* 225.0/227.0 [M + H]⁺. A pressure bottle was charged with 8-bromoquinazolin-4(3H)-one (1.50 g, 6.67 mmol), Pd(PPh₃)₄ (0.770 g, 0.667 mmol), zinc cyanide (2.348 g, 20.00 mmol), and DMF (26.7 mL). The bottle was sealed, and the mixture was heated at 100 °C for 24 h. The mixture was poured into water, and the resulting solids were filtered, washed with water, and dried. This material was triturated in DCM, filtered, washed with DCM, and dried. Solids also precipitated out of the aqueous filtrate and were filtered, washed with water, and dried. The solids were combined to provide the desired compound as a white solid. The material was used without further purification. MS, *m/z* 172.0 [M + H]⁺.

Pyrido[2,3-*d*]pyrimidin-4(3H)-one (**39j**). The title compound was prepared according to general procedure F using 2-aminonicotinic acid as a tan solid in 49% yield. ¹H NMR (400 MHz, DMSO-*d*₆) δ 12.40 (br s, 1H), 8.95 (dd, *J* = 2.05, 4.60 Hz, 1H), 8.50 (dd, *J* = 2.05, 7.92 Hz, 1H), 8.31 (s, 1H), 7.55 (dd, *J* = 4.60, 7.92 Hz, 1H). MS, *m/z* 147.9 [M + H]⁺.

7-Methyl-1H-purin-6(7H)-one (**39l**). A pressure bottle was charged with 6-chloro-7-methyl-7H-purine²¹ (2.12 g, 12.58 mmol), dioxane (50 mL), and hydrochloric acid (2 M in dioxane, 12.58 mL, 25.2 mmol), and the reaction was stirred at 90 °C for 2 h. The mixture was concentrated to provide the title compound as the hydrochloride salt (2.4 g, 12.9 mmol, 100% yield) as a tan solid. ¹H NMR (400 MHz, DMSO-*d*₆) δ 8.61 (s, 1H), 8.10 (s, 1H), 4.01 (s, 3H). MS, *m/z* 151.0 [M + H]⁺.

2-Bromo-*N*-(4-chlorophenethyl)acetamide (**40**). To a solution of bromoacetic acid (4.46 g, 32.1 mmol) in 40.0 mL of EtOAc at 0 °C was added 1-propanephosphonic acid cyclic anhydride, 50 wt % in EtOAc (30.7 mL, 48.2 mmol). To the resulting mixture was added a solution of 2-(4-chlorophenyl)ethanamine (4.50 mL, 32.1 mmol) and triethylamine (8.96 mL, 64.3 mmol) in EtOAc (20.0 mL). The resulting mixture was stirred at room temperature overnight. The mixture was washed twice with water and brine and was dried over Na₂SO₄. The solvents were removed in vacuo. The crude material was absorbed onto a plug of silica gel and purified by chromatography, eluting with 0% to 50% EtOAc/heptane, to provide the title compound (5.1 g, 18.44 mmol, 57% yield) as a white solid. ¹H NMR (400 MHz, DMSO-*d*₆) δ 8.32 (br s, 1H), 7.30–7.39 (m, 2H), 7.20–7.27 (m, 2H), 3.81 (s, 2H), 3.25–3.31 (m, 2H), 2.71 (t, *J* = 7.14 Hz, 2H). MS, *m/z* 275.7/277.7 [M + H]⁺.

2-(8-Methyl-4-oxoquinazolin-3(4H)-yl)acetic Acid (**41a**). A pressure bottle was charged with 8-methylquinazolin-4(3H)-one (**39a**) (2.88 g, 17.98 mmol), potassium carbonate (3.73 g, 27.0 mmol), DMF (71.9 mL), and methyl 2-bromoacetate (2.04 mL, 21.58 mmol), and the mixture was stirred at 50 °C for 1.5 h. The mixture was poured into water, and the resulting solids were filtered, washed with water, and air-dried to provide the title compound (3.501 g, 15.08 mmol, 84% yield) as an off-white solid. ¹H NMR (400 MHz, DMSO-*d*₆) δ 8.36–8.41 (m, 1H), 7.95–8.01 (m, 1H), 7.70–7.75 (m, 1H), 7.42–7.49 (m, 1H), 4.84 (s, 2H), 3.71 (s, 3H), 2.56 (s, 3H). MS, *m/z* 233.0 [M + H]⁺. A round-bottom flask was charged with methyl 2-(8-methyl-4-oxoquinazolin-3(4H)-yl)acetate (3.5 g, 15.07 mmol), THF (22.61 mL), water (7.54 mL), and LiOH (1.805 g, 75 mmol), and the mixture was stirred at RT for 1 h. The mixture was brought to pH 2 by addition of 2 N HCl and was extracted twice with EtOAc. The combined organic portions were dried over sodium sulfate, filtered, and concentrated. Solids remained in the aqueous layer, which were filtered, washed with water, and dried. The solids from the organic and aqueous portions were combined and dried under high vacuum to provide the desired compound (3.01 g, 13.79 mmol, 92% yield) as a tan solid. ¹H NMR (400 MHz, DMSO-*d*₆) δ 13.19 (br s, 1H), 8.30–8.45 (m, 1H), 7.94–8.04 (m, 1H), 7.67–7.76 (m, 1H), 7.38–7.50 (m, 1H), 4.66–4.81 (m, 2H), 2.55 (s, 3H). MS, *m/z* 219.0 [M + H]⁺.

2-(4-Oxoquinazolin-3(4H)-yl)acetic Acid (**41b**). A vial was charged with quinazolin-4(3H)-one (**39b**) (1.00 g, 6.84 mmol), K₂CO₃ (1.419 g, 10.26 mmol), DMF (13.68 mL), and methyl 2-bromoacetate (0.696 mL, 7.53 mmol), and the mixture was heated at 50 °C for 4 h. Water and EtOAc were added, and the layers were separated. The organic portion was dried over sodium sulfate, filtered, and concentrated. The crude material was dried under high vacuum to provide methyl 2-(4-oxoquinazolin-3(4H)-yl)acetate as a white solid (1.3 g, 5.96 mmol, 87% yield). ¹H NMR (400 MHz, DMSO-*d*₆) δ ppm 8.35–8.39 (m, 1 H), 8.12–8.17 (m, 1 H), 7.84–7.90 (m, 1 H), 7.69–7.74 (m, 1 H), 7.55–7.61 (m, 1 H), 4.85 (s, 2 H), 3.71 (s, 3 H). MS, *m/z* 219.0 [M + H]⁺. A round-bottom flask was charged with methyl 2-(4-oxoquinazolin-3(4H)-yl)acetate (500 mg, 2.291 mmol), THF (6.8 mL), water (0.31 mL), and LiOH (549 mg, 22.91 mmol). The mixture was stirred overnight at RT. The mixture was brought to acidic pH with 2 N HCl, and EtOAc was added. The layers were separated, and the organic portion was dried over sodium sulfate, filtered, and concentrated to provide the title compound as a white solid (410 mg,

2.00 mmol, 88% yield). ^1H NMR (400 MHz, $\text{DMSO}-d_6$) δ ppm 13.14–13.23 (m, 1 H), 8.34–8.37 (m, 1 H), 8.12–8.18 (m, 1 H), 7.83–7.89 (m, 1 H), 7.69–7.73 (m, 1 H), 7.52–7.61 (m, 1 H), 4.70–4.75 (m, 2 H). MS, m/z 205.0 $[\text{M} + \text{H}]^+$.

2-(4-Oxo-8-(trifluoromethyl)quinazolin-3(4H)-yl)acetic Acid (41c). A vial was charged with 8-(trifluoromethyl)quinazolin-4(3H)-one (**39f**) (0.200 mg, 0.93 mmol), potassium carbonate (0.19 mg, 1.40 mmol), methyl 2-bromoacetate (0.11 mL, 1.12 mmol), and DMF (1.9 mL). The mixture was heated at 50 °C for 2 h. Water and EtOAc were added, and the layers were separated. The organic portion was dried over sodium sulfate, filtered, and concentrated. The crude material was purified by silica gel chromatography, using 15–70% EtOAc/heptane to provide methyl 2-(4-oxo-8-(trifluoromethyl)quinazolin-3(4H)-yl)-acetate (0.160 g, 0.559 mmol, 59.9% yield) as a light yellow solid. ^1H NMR (400 MHz, $\text{DMSO}-d_6$) δ 8.52 (s, 1H), 8.40–8.47 (m, 1H), 8.25 (d, J = 7.63 Hz, 1H), 7.72 (t, J = 7.92 Hz, 1H), 4.88 (s, 2H), 3.68–3.77 (m, 3H). MS, m/z 287.0 $[\text{M} + \text{H}]^+$. Methyl 2-(4-oxo-8-(trifluoromethyl)quinazolin-3(4H)-yl)-acetate (0.160 g, 0.559 mmol) and LiOH (0.062 g, 2.80 mmol) were added to water (0.28 mL) and THF (0.84 mL). The mixture was stirred at room temperature for 1 h. The mixture was brought to pH 2 by addition of 2 N HCl and was extracted twice with EtOAc. The combined organics were dried over sodium sulfate, filtered, and concentrated to yield (130 mg, 0.478 mmol, 85% yield) as an off-white solid. ^1H NMR (400 MHz, $\text{DMSO}-d_6$) δ 13.32 (br s, 1H), 8.49–8.55 (m, 1H), 8.43 (dd, J = 0.98, 8.02 Hz, 1H), 8.19–8.29 (m, 1H), 7.66–7.78 (m, 1H), 4.69–4.85 (m, 2H). MS, m/z 273.0 $[\text{M} + \text{H}]^+$.

2-(8-Fluoro-4-oxoquinazolin-3(4H)-yl)acetic Acid (41d). A vial was charged with 8-fluoroquinazolin-4(3H)-one (**39g**) (0.200 g, 1.22 mmol), potassium carbonate (0.25 g, 1.83 mmol), methyl 2-bromoacetate (0.14 mL, 1.46 mmol), and DMF (2.4 mL). The mixture was heated at 50 °C for 2 h. The mixture was poured into water, and the resulting solids were filtered, washed with water, and dried to provide methyl 2-(8-fluoro-4-oxoquinazolin-3(4H)-yl)-acetate (0.170 g, 0.720 mmol, 59.1% yield) as a light yellow solid. ^1H NMR (400 MHz, $\text{DMSO}-d_6$) δ 8.52 (s, 1H), 8.40–8.47 (m, 1H), 8.25 (d, J = 7.63 Hz, 1H), 7.72 (t, J = 7.92 Hz, 1H), 4.88 (s, 2H), 3.68–3.77 (m, 3H). MS, m/z 287.0 $[\text{M} + \text{H}]^+$. Methyl 2-(8-fluoro-4-oxoquinazolin-3(4H)-yl)-acetate (0.170 g, 0.720 mmol) and LiOH (0.086 g, 3.60 mmol) were added to water (0.36 mL) and THF (1.08 mL). The mixture was stirred at room temperature for 1 h. The mixture was brought to pH 2 by addition of 2 N HCl and was extracted twice with EtOAc. The combined organics were dried over sodium sulfate, filtered, and concentrated to yield the title compound (110 mg, 0.495 mmol, 69% yield) as an off-white solid. ^1H NMR (400 MHz, $\text{DMSO}-d_6$) δ ppm 13.14–13.35 (m, 1 H), 8.42 (s, 1 H), 7.90–8.04 (m, 1 H), 7.68–7.81 (m, 1 H), 7.41–7.61 (m, 1 H), 4.76 (s, 2 H). MS, m/z 223.0 $[\text{M} + \text{H}]^+$.

2-(4-Oxopyrido[2,3-d]pyrimidin-3(4H)-yl)acetic Acid Hydrochloride (41e). A vial was charged with pyrido[2,3-d]pyrimidin-4(3H)-one (**39j**) (5.00 g, 34.0 mmol), potassium carbonate (7.04 g, 51.0 mmol), *tert*-butyl bromoacetate (5.94 mL, 40.8 mmol), and DMF (34 mL). The mixture was heated at 70 °C for 1 h. Water and EtOAc were added, and the layers were separated. The organic portion was dried with sodium sulfate, filtered, and concentrated. The crude material was purified by silica gel chromatography, 25–100% 90/10 DCM/MeOH in DCM, to provide *tert*-butyl 2-(4-oxopyrido[2,3-d]pyrimidin-3(4H)-yl)-acetate (7.2 g, 27.6 mmol, 81.0% yield) as a light yellow solid. ^1H NMR (400 MHz, $\text{DMSO}-d_6$) δ 9.00 (dd, J = 2.01, 4.55 Hz, 1H), 8.58 (s, 1H), 8.56 (dd, J = 2.05, 7.92 Hz, 1H), 7.61 (dd, J = 4.60, 7.92 Hz, 1H), 4.74 (s, 2H), 1.41–1.47 (m, 9H). MS, m/z 261.8 $[\text{M} + \text{H}]^+$. *tert*-Butyl 2-(4-oxopyrido[2,3-d]pyrimidin-3(4H)-yl)-acetate (7.2 g, 27.6 mmol) was dissolved in dichloromethane (55.1 mL). Hydrochloric acid (2 N in dioxane, 11.31 mL, 138.0 mmol) was added, and the reaction was stirred at RT for 30 min. The reaction mixture was concentrated in vacuo to provide the desired product (4.9 g, 74%) as a light yellow solid. ^1H NMR (400 MHz, $\text{DMSO}-d_6$) δ 9.01 (dd, J = 2.05, 4.60 Hz, 1H), 8.62 (s, 1H), 8.60 (dd, J = 2.05, 7.92 Hz, 1H), 7.64 (dd, J = 4.60, 7.92 Hz, 1H), 4.77 (s, 2H). MS, m/z 206.0 $[\text{M} + \text{H}]^+$.

2-(7-Methyl-6-oxo-6,7-dihydro-1H-purin-1-yl)acetic Acid Hydrochloride (41f). A vial was charged with 7-methyl-1H-purin-6(7H)-one (**39l**) (180 mg, 1.199 mmol), potassium carbonate (199 mg, 1.439 mmol), *tert*-butyl bromoacetate (0.175 mL, 1.199 mmol), and DMF (2.40 mL). The mixture was heated at 50 °C for 6 h. Water and EtOAc were added, and the layers were separated. The organic portion was dried with sodium sulfate, filtered, and concentrated. The crude material was purified by silica gel chromatography, 0–40% 90/10 DCM/MeOH in DCM, to provide *tert*-butyl 2-(7-methyl-6-oxo-6,7-dihydro-1H-purin-1-yl)-acetate (110 mg, 0.416 mmol, 34.7% yield) as a white foamy solid. ^1H NMR (400 MHz, $\text{DMSO}-d_6$) δ 8.22–8.27 (m, 1H), 8.16–8.21 (m, 1H), 4.66–4.76 (m, 2H), 3.92–4.01 (m, 3H), 1.39–1.48 (m, 9H). MS, m/z 265.0 $[\text{M} + \text{H}]^+$. *tert*-Butyl 2-(7-methyl-6-oxo-6,7-dihydro-1H-purin-1-yl)-acetate (110 mg, 0.416 mmol) was dissolved in concentrated HCl in a vial and stirred at RT. After 30 min, the mixture was concentrated and the title compound (86 mg, 0.413 mmol, 99% yield) was isolated as an off-white solid. ^1H NMR (400 MHz, $\text{DMSO}-d_6$) δ 8.52 (s, 1H), 8.34–8.38 (m, 1H), 4.76 (s, 2H), 3.97–4.02 (m, 3H). MS, m/z 209.0 $[\text{M} + \text{H}]^+$.

2-(4-Oxopyrido[2,3-d]pyrimidin-3(4H)-yl)acetonitrile (42a). A vial was charged with pyrido[2,3-d]pyrimidin-4(3H)-one (**39j**) (150 mg, 1.019 mmol), potassium carbonate (211 mg, 1.529 mmol), bromoacetonitrile (0.071 mL, 1.070 mmol), and DMF (4.08 mL). The reaction was stirred at 50 °C for 1 h. Water and EtOAc were added, and the layers were separated. The organic portion was dried with sodium sulfate, filtered, and concentrated, to provide the desired compound (96 mg, 51% yield). ^1H NMR (400 MHz, $\text{DMSO}-d_6$) δ 9.01 (dd, J = 2.05, 4.60 Hz, 1H), 8.62–8.65 (m, 1H), 8.60 (dd, J = 2.05, 7.92 Hz, 1H), 7.63 (dd, J = 4.60, 7.92 Hz, 1H), 5.08–5.15 (m, 2H). MS, m/z 187.0 $[\text{M} + \text{H}]^+$.

2-(7-Methyl-6-oxo-6,7-dihydro-1H-purin-1-yl)acetonitrile (42b). 7-Methyl-1H-purin-6(7H)-one hydrochloride (**39l**) (900 mg, 4.82 mmol), potassium carbonate (1666 mg, 12.06 mmol), DMF (19.300 mL), and bromoacetonitrile (0.336 mL, 4.82 mmol) were stirred at 55 °C for 2 h. Upon cooling to RT, water and DCM were added. The layers were extracted, and the aqueous portion was extracted again with DCM. The combined organic portions were dried over sodium sulfate, filtered, and concentrated to provide the title compound (260 mg, 1.374 mmol, 29% yield) as a white solid. ^1H NMR (400 MHz, $\text{DMSO}-d_6$) δ ppm 8.34–8.37 (m, 1 H), 8.20–8.26 (m, 1 H), 5.09–5.12 (m, 2 H), 3.96–4.00 (s, 3 H). MS, m/z 190.0 $[\text{M} + \text{H}]^+$.

(Z)-N'-Hydroxy-2-(4-oxopyrido[2,3-d]pyrimidin-3(4H)-yl)-acetimidamide (43a). A vial was charged with 2-(4-oxopyrido[2,3-d]pyrimidin-3(4H)-yl)-acetonitrile (**42a**) (96 mg, 0.516 mmol), EtOH (2.06 mL), and hydroxylamine (0.126 mL, 2.063 mmol). The heterogeneous mixture was stirred at 80 °C for 1 h. Upon cooling, the solids were filtered, washed with EtOH, and dried under high vacuum to provide the title compound (72 mg, 0.328 mmol, 63.7% yield) as a rust-colored solid. ^1H NMR (400 MHz, $\text{DMSO}-d_6$) δ 9.16–9.27 (m, 1H), 8.92–9.01 (m, 1H), 8.52–8.57 (m, 1H), 8.48–8.52 (m, 1H), 7.53–7.61 (m, 1H), 5.64–5.77 (m, 2H), 4.57–4.71 (m, 2H). MS, m/z 219.9 $[\text{M} + \text{H}]^+$.

(Z)-N'-Hydroxy-2-(7-methyl-6-oxo-6,7-dihydro-1H-purin-1-yl)-acetimidamide (43b). A vial was charged with 2-(7-methyl-6-oxo-6,7-dihydro-1H-purin-1-yl)-acetonitrile (**42b**) (260 mg, 1.374 mmol), EtOH (5498 μL), and hydroxylamine (337 μL , 5.50 mmol). The reaction mixture was heated at 80 °C for 2 h. Upon cooling to RT, water was added, and the solids were filtered, washed with water, and dried. The title compound (145 mg, 0.653 mmol, 47.5% yield) was isolated as a tan solid. ^1H NMR (400 MHz, $\text{DMSO}-d_6$) δ ppm 9.17–9.21 (m, 1 H), 8.14–8.19 (m, 2 H), 5.59–5.66 (m, 2 H), 4.59–4.64 (m, 2 H), 3.93–3.98 (m, 3 H). MS, m/z 223.2 $[\text{M} + \text{H}]^+$.

3-(4-Chlorophenyl)butanoic Acid (45). To a round-bottom flask was added a spatula tip of Raney nickel (slurry in water) followed by a solution of (E)-ethyl 3-(4-chlorophenyl)but-2-enoate (prepared in step 1, intermediate **47**) (700 mg, 3.12 mmol) dissolved in 6 mL of EtOH. The flask was evacuated and filled with hydrogen. The reaction was stirred at 20 °C for 18 h under hydrogen atmosphere. The mixture was passed through a pad of Celite and rinsed with EtOH. The filtrate was concentrated, and the crude material was purified via reverse phase

chromatography using a gradient of 50–100% acetonitrile (0.1% TFA):water (0.1% TFA). The product containing fractions were combined and brought to pH 8 with saturated NaHCO_3 . The aqueous portion was extracted into ethyl acetate, dried with sodium sulfate, filtered through a fritted funnel, and concentrated to yield ethyl 3-(4-chlorophenyl)butanoate (160 mg, 0.706 mmol, 23% yield) as a light yellow oil. ^1H NMR (400 MHz, $\text{DMSO}-d_6$) δ 7.24–7.36 (m, 4H), 3.94–4.01 (m, 2H), 3.13–3.20 (m, 1H), 2.58 (dd, $J = 4.21, 7.53$ Hz, 2H), 1.17–1.21 (m, 3H), 1.09 (t, $J = 7.09$ Hz, 3H). MS, m/z 227.0 $[\text{M} + \text{H}]^+$. A round-bottom flask was charged with ethyl 3-(4-chlorophenyl)butanoate (160 mg, 0.706 mmol), THF (1.06 mL), water (0.353 mL), and LiOH (85 mg, 3.53 mmol). The mixture was stirred at RT for 2 h, brought to pH 2 by addition of 2 N HCl, and extracted twice with EtOAc. The combined organic portions were dried over sodium sulfate, filtered, and concentrated to yield the title compound (120 mg, 0.604 mmol, 86% yield) as an off-white solid. ^1H NMR (400 MHz, $\text{DMSO}-d_6$) δ 12.03 (s, 1H), 7.23–7.36 (m, 4H), 3.06–3.22 (m, 1H), 2.47–2.50 (m, 2H), 1.19 (d, $J = 6.94$ Hz, 3H). MS, m/z 199.0 $[\text{M} + \text{H}]^+$.

(E)-3-(4-Chlorophenyl)but-2-enoic Acid (47). In a 100 mL round-bottom flask NaH (60% dispersion in mineral oil) (168 mg, 4.20 mmol) were dissolved in 9 mL of THF and triethyl phosphonoacetate (0.798 mL, 3.56 mmol) was added dropwise. In a separate flask, 4'-chloroacetophenone (500 mg, 3.23 mmol) was dissolved in 4 mL of THF and added quickly to the phosphonate mixture. The reaction was stirred for 30 min at RT, cooled to 0 °C, and diluted with methanol. Saturated ammonium chloride was slowly added until a precipitate formed. The solids were filtered and rinsed with ethyl acetate. Water was added to the filtrate, and the layers were separated. The organic portion was dried with sodium sulfate, filtered, and concentrated. The crude material was purified with reverse phase chromatography using a gradient of 50–100% acetonitrile (0.1% TFA):water (0.1% TFA). The product containing fractions were brought to pH 8 with saturated NaHCO_3 . The aqueous portion was extracted into ethyl acetate, dried with sodium sulfate, filtered through a fritted funnel, and concentrated to yield (E)-ethyl 3-(4-chlorophenyl)but-2-enoate (220 mg, 0.979 mmol 30.3% yield) as a colorless oil. ^1H NMR (400 MHz, chloroform- d) δ 7.38–7.46 (m, 2H), 7.32–7.38 (m, 2H), 6.09–6.15 (m, 1H), 4.16–4.27 (m, 2H), 2.52–2.61 (m, 3H), 1.33 (t, $J = 7.14$ Hz, 3H). MS, m/z 225.0 $[\text{M} + \text{H}]^+$. A round-bottom flask was charged with (E)-ethyl 3-(4-chlorophenyl)but-2-enoate (100 mg, 0.445 mmol), THF (668 μL), water (223 μL), and LiOH (53.3 mg, 2.225 mmol), and the mixture was stirred at RT for 17 h. The mixture was brought to pH 2 by addition of 2 N HCl and was extracted twice with EtOAc. The combined organic portions were dried over sodium sulfate, filtered, and concentrated to yield the desired compound as an off-white solid. MS, m/z 197.0 $[\text{M} + \text{H}]^+$.

(3-(4-Chlorophenethyl)-1,2,4-oxadiazol-5-yl)methanamine (48). A vial was charged with *N*-Boc-glycine (441 mg, 2.52 mmol), (Z)-3-(4-chlorophenyl)-*N'*-hydroxypropanimidamide (50a) (500 mg, 2.52 mmol), triethylamine (1.75 mL, 12.58 mmol), and EtOAc (5.03 mL). 1-Propanephosphonic acid cyclic anhydride, 50 wt % solution in ethyl acetate (4.00 mL, 6.29 mmol) was added, and the mixture was stirred at 80 °C for 5 h. Water and EtOAc were added, and the layers were separated. The organic portion was dried over sodium sulfate, filtered, and concentrated. The crude material was purified by silica gel chromatography (Isolera), 0–50% EtOAc/heptane, to provide *tert*-butyl ((3-(4-chlorophenethyl)-1,2,4-oxadiazol-5-yl)methyl)carbamate (487 mg, 1.442 mmol, 57.3% yield) as a colorless oil. ^1H NMR (400 MHz, chloroform- d) δ 7.24–7.29 (m, 2H), 7.12–7.17 (m, 2H), 5.14 (br s, 1H), 4.49–4.63 (m, 2H), 2.95–3.13 (m, 4H), 1.48 (s, 9H). MS, m/z 360.0 $[\text{M} + \text{Na}]^+$. A vial was charged with *tert*-butyl ((3-(4-chlorophenethyl)-1,2,4-oxadiazol-5-yl)methyl)carbamate (480 mg, 1.421 mmol), DCM (2.84 mL) and TFA (1.10 mL, 14.21 mmol), and the mixture was stirred at RT overnight. The mixture was concentrated, dissolved in DCM, and washed with saturated NaHCO_3 . The organic portion was dried over sodium sulfate, filtered, and concentrated. The title compound (290 mg, 1.220 mmol, 86% yield) was isolated as a tan solid. ^1H NMR (400 MHz, $\text{DMSO}-d_6$) δ 7.30–

7.36 (m, 2H), 7.22–7.30 (m, 2H), 3.91 (s, 2H), 2.94–3.02 (m, 4H), 2.00–2.09 (m, 2H). MS, m/z 238.0 $[\text{M} + \text{H}]^+$.

3-(6-Chloropyridin-3-yl)propanenitrile (49b). A round-bottom flask was charged with diethyl cyanomethylphosphonate (1.50 g, 8.48 mmol) in THF (14.1 mL). NaH (60% dispersion, 0.339 g, 8.48 mmol) was added, and the mixture was stirred at RT for 10 min until gas evolution ceased. After cooling to 0 °C, 6-chloronicotinaldehyde (1.00 g, 7.06 mmol) was added, and the reaction was allowed to warm to RT. EtOAc and water were added, and the layers were separated. The organic portion was dried over sodium sulfate, filtered, and concentrated. The crude material was triturated in diethyl ether, filtered, washed with diethyl ether, and dried to provide (E)-3-(6-chloropyridin-3-yl)acrylonitrile (500 mg, 3.04 mmol, 43.0% yield) as an off-white solid. ^1H NMR (400 MHz, chloroform- d) δ 8.48 (d, $J = 2.54$ Hz, 1H), 7.76 (dd, $J = 2.54, 8.31$ Hz, 1H), 7.42 (d, $J = 24$ Hz, 1H), 7.40 (d, $J = 1.76$ Hz, 1H), 5.97 (d, $J = 16.73$ Hz, 1H). MS, m/z 165.0 $[\text{M} + \text{H}]^+$. A vial was charged with (E)-3-(6-chloropyridin-3-yl)acrylonitrile (300 mg, 1.823 mmol), pyridine (5.47 mL), and MeOH (1.82 mL). NaBH_4 (103 mg, 2.73 mmol) was added, and the mixture was heated at 70 °C for 2 h. EtOAc and saturated NH_4Cl were added, and the layers were separated. The organic portion was dried over sodium sulfate, filtered, and concentrated. The crude material was purified by silica gel chromatography, 0–50% EtOAc/heptane, to give the title compound (90 mg, 0.540 mmol, 29.6% yield) as a yellow oil. MS, m/z 167.0 $[\text{M} + \text{H}]^+$.

3-(4-Chlorophenyl)-3-hydroxypropanenitrile (49c). A round-bottom flask was charged with 3-(4-chlorophenyl)-3-oxopropanenitrile (1.0 g, 5.57 mmol) and EtOH (11.14 mL). The solution was cooled to 0 °C, and sodium borohydride (0.421 g, 11.14 mmol) was added. After stirring at 0 °C for 1 h, the reaction was quenched with saturated ammonium chloride and the ice bath was removed. The reaction was extracted into dichloromethane, washed with water and brine, dried over sodium sulfate, filtered, and concentrated. The crude material was purified by silica gel chromatography, using a gradient of 10–75% 90/10 DCM/MeOH in DCM, to provide the desired compound (0.80 g, 4.40 mmol, 79% yield) as a colorless oil. ^1H NMR (400 MHz, $\text{DMSO}-d_6$) δ 7.39–7.47 (m, 4H), 6.03 (d, $J = 4.50$ Hz, 1H), 4.86–4.96 (m, 1H), 2.86–2.95 (m, 1H), 2.78–2.86 (m, 1H). MS, m/z 204.0 $[\text{M} + \text{Na}]^+$.

(E)-3-(4-Chlorophenyl)but-2-enenitrile (49d). A vial was charged with diethyl cyanomethylphosphonate (2.52 mL, 14.23 mmol) and THF (25.9 mL). NaH (60% dispersion) (0.569 g, 14.23 mmol) was added, and the reaction was stirred at room temperature for 10 min. 4'-Chloroacetophenone (1.681 mL, 12.94 mmol) was added and the reaction stirred for 1 h. EtOAc and saturated NH_4Cl were added, and the layers were separated. The aqueous phase was extracted with EtOAc, and the combined organic portions were dried over MgSO_4 , filtered, and concentrated. The crude material was purified via silica gel column chromatography, eluting with 0–50% EtOAc/heptane. The product containing fractions were combined and concentrated in vacuo to yield the desired compound (2.25 g, 98% yield). MS, m/z 178.2 $[\text{M} + \text{H}]^+$.

(Z)-3-(4-Chlorophenyl)-*N'*-hydroxypropanimidamide (50a). A pressure bottle was charged with 3-(4-chlorophenyl)propionitrile (49a) (2.0 mL, 12.08 mmol), EtOH (24.15 mL), and hydroxylamine (3.19 mL, 48.3 mmol). The mixture was stirred at 80 °C for 1.5 h. Upon cooling to RT, water was added and the mixture was allowed to stand. The mixture was poured onto ice, which caused precipitation. The solids were filtered, washed with water, and dried to provide the title compound (2.23 g, 11.23 mmol, 93% yield) as a white solid. ^1H NMR (400 MHz, $\text{DMSO}-d_6$) δ 8.70–8.76 (m, 1H), 7.29–7.35 (m, 2H), 7.20–7.27 (m, 2H), 5.41 (s, 2H), 2.73–2.83 (m, 2H), 2.17–2.25 (m, 2H). MS, m/z 199.0 $[\text{M} + \text{H}]^+$.

(Z)-3-(6-Chloropyridin-3-yl)-*N'*-hydroxypropanimidamide (50b). A vial was charged with 3-(6-chloropyridin-3-yl)propanenitrile (49b) (90 mg, 0.540 mmol), EtOH (2.16 mL), and hydroxylamine (0.132 mL, 2.161 mmol), and the mixture was stirred at 45 °C for 24 h. Water and EtOAc were added, the layers were separated, and the organic portion was dried over sodium sulfate, filtered, and concentrated to give the desired product (93 mg, 0.466 mmol, 86% yield) as a slightly

yellow oil. ^1H NMR (400 MHz, $\text{DMSO}-d_6$) δ 8.70–8.81 (m, 1H), 8.19–8.32 (m, 1H), 7.71 (dd, $J = 2.54, 8.22$ Hz, 1H), 7.36–7.46 (m, 1H), 5.43 (s, 2H), 2.73–2.90 (m, 2H), 2.18–2.32 (m, 2H). MS, m/z 200.0 $[\text{M} + \text{H}]^+$.

(Z)-3-(4-Chlorophenyl)-N'-3-dihydroxypropanimidamide (50c). A vial was charged with 3-(4-chlorophenyl)-3-hydroxypropanenitrile (49c) (200 mg, 1.101 mmol), EtOH (2.20 mL), and hydroxylamine (0.270 mL, 4.40 mmol). The solution was stirred at 80 °C for 1 h. Upon cooling to RT, the EtOH was evaporated under reduced pressure. Water and EtOAc were added, and the layers were separated. The organic portion was dried over sodium sulfate, filtered, and concentrated to yield the desired product (172 mg, 0.801 mmol, 72.8% yield) as a light yellow waxy solid. ^1H NMR (400 MHz, $\text{DMSO}-d_6$) δ 8.76 (s, 1H), 7.32–7.37 (m, 4H), 5.35–5.43 (m, 2H), 4.81–4.91 (m, 1H), 3.12–3.19 (m, 1H), 2.26–2.34 (m, 1H), 2.18–2.26 (m, 1H). MS, m/z 215.0 $[\text{M} + \text{H}]^+$.

(1Z,2E)-3-(4-Chlorophenyl)-N'-hydroxybut-2-enimidamide (50d). (E)-3-(4-chlorophenyl)but-2-enitrile (49d) (2.25 g, 12.67 mmol) was added to a microwave vial followed by EtOH (50.7 mL) and hydroxylamine (0.776 mL, 12.67 mmol). The vial was capped and heated to 100 °C in the microwave reactor for 1 h. The solvent was removed in vacuo to provide the title compound (2.45 g, 92% yield) as an off-white solid. ^1H NMR (400 MHz, $\text{DMSO}-d_6$) δ 9.39–9.42 (m, 1H), 7.47–7.52 (m, 2H), 7.39–7.44 (m, 2H), 6.03–6.12 (m, 1H), 5.49 (s, 2H), 2.28 (d, $J = 1.37$ Hz, 3H). MS, m/z 211.2 $[\text{M} + \text{H}]^+$.

3-(4-Chlorophenyl)propanehydrazide (51). A pressure bottle was charged with methyl 3-(4-chlorophenyl)propanoate (1.05 g, 5.29 mmol), EtOH (10.57 mL) and hydrazine hydrate (2.62 mL, 52.9 mmol). The bottle was sealed, and the mixture was heated at 100 °C for 17 h. A small amount of water was added, and the mixture was allowed to stand at RT. Crystals formed, which were filtered, washed with water, and dried. The title compound (685 mg, 3.45 mmol, 65.2% yield) as isolated as a white solid. ^1H NMR (400 MHz, $\text{DMSO}-d_6$) δ ppm 8.89–8.98 (m, 1 H), 7.28–7.35 (m, 2 H), 7.23 (s, 2 H), 4.10–4.17 (m, 2 H), 2.73–2.84 (m, 2 H), 2.26–2.34 (m, 2 H). MS, m/z 199.0 $[\text{M} + \text{H}]^+$.

TRPA1 Calcium Flux Cell Assays. The generation of CHO cell lines stably expressing human and rat TRPA1 in tetracycline-inducible T-REx expression systems (Gibco-Invitrogen, Carlsbad, CA) was previously described.²³ Both human and rat TRPA1 cell lines were maintained in Ham's F-12 nutrient mix (Gibco-Invitrogen) containing 10% tetracycline-screened fetal bovine serum (Hyclone, Logan, UT), 1% penicillin/streptomycin/glutamine solution (Gibco-Invitrogen), 10 mg/mL blasticidin S HCl (Gibco-Invitrogen), 250 mg/mL zeocin (Gibco-Invitrogen), and 400 mg/mL geneticin (Gibco-Invitrogen). Intracellular calcium flux was measured with the Fluo-4 NW (no-wash) fluorescent calcium-sensing dye (Molecular Probes, Eugene, OR) and the FLIPR Tetra fluorescence kinetic plate reader (Molecular Devices, Sunnyvale CA). Twenty-four hours before dye-loading, cells were seeded 20000 cells/well in 384-well flat clear-bottom black assay plates (Costar, Corning, NY) in culture media supplemented with 0.5 mg/mL tetracycline (Corning, Manassas, VA). Fluo-4 NW dye and water-soluble probenecid (Gibco-Invitrogen) were reconstituted with assay buffer (Hank's Balanced Salt Solution with 20% HEPES, Gibco-Invitrogen). Culture media was removed before the addition of reconstituted dye to the cell plates. Cells were incubated with the dye at 37 °C for 30 min before equilibrating at room temperature for an additional 30 min. Two additions were conducted on the FLIPR Tetra to measure in-sequence agonist and antagonist activity. Test compounds were added in the first addition, and agonist activity data were collected for 2 min. An EC_{90} concentration (3 μM for human TRPA1 and 35 μM for rat TRPA1) of TRPA1 agonist allyl isothiocyanate (AITC) (Fluka-Sigma-Aldrich, St. Louis, MO) was then added, and antagonist activity was measured for a further 2 min of data collection. Data were analyzed with Screener (Genedata AG, Basel, Switzerland) data analysis software. The amount of signal generated in the presence of compounds versus that in the presence of low control (DMSO vehicle alone) and high control (for agonists, a saturating concentration of AITC, 15 μM for human TRPA1, and 200 μM for rat TRPA1; for antagonists, an EC_{90} concentration of AITC) was

calculated using the formula: % control (POC) = (compound – average low)/(average high – average low) \times 100. For IC_{50} determination, data were fitted to a four-parameter equation ($y = A + ((B - A)/(1 + ((x/C)^D)))$), where A is the minimum y (POC) value, B is the maximum y (POC), C is the x (compound concentration) at the point of inflection, and D is the slope factor).

⁴⁵Ca²⁺ Assays (rTRPA1, hTRPA1, antagonist and agonist mode). These assays were run according to the published procedures.^{22,23}

hTRPV1, hTRPV4, rTRPV3, rTRPM8 Assays. These assays were run according to the published procedure.²³

Antagonist against Methylglyoxal (MG) Assay. Cells were generated and maintained as described for the TRPA1 calcium flux assays. On the day of assay, culture media was removed and cells were incubated for 10 min at RT with 50 μL of compound in compound dilution buffer (HBSS containing 1 mM HEPES + 0.1 mg/mL BSA) at final concentrations (2.0 nM to 40 μM , 1:3 ratio) prior to the addition 50 μL of agonist (MG at final concentration 2.74 mM) and radioactive calcium (final concentration 10 $\mu\text{Ci/mL}$) in assay buffer (Ham's F-12 containing 15 mM HEPES + 0.1% BSA), followed by another 3 min incubation at RT. The reaction mixture was aspirated, and cells were washed three times with phosphate buffer saline (PBS) containing 0.1 mg/mL BSA. Radioactivity was measured using a TopCount microplate scintillation counter. The activation of TRPA1 was measured by the cellular uptake of radioactive calcium. The agonist (MG)-induced ⁴⁵Ca²⁺ uptake was considered as 100%, and the wells with radioactive assay buffer without agonist were taken as 0%.

Antagonist against Hypotonicity Assay. Cells were generated and maintained as described for the TRPA1 calcium flux assays. On the day of assay, culture media was removed and cells were incubated for 10 min at RT with 20 μL of compound in normal assay buffer (Ham's F-12 containing 15 mM HEPES + 0.1% BSA) at final concentrations (2.0 nM to 40 μM , 1:3 ratio) prior to the addition 80 μL of Hypo-Osmolarity buffer (50 mOsmol/L, diluted assay buffer, at a final osmolarity 100 mOsmol) with radioactive calcium (final concentration 10 $\mu\text{Ci/mL}$), followed by another 3 min incubation at RT. The reaction mixture was aspirated, and cells were washed three times with phosphate buffer saline (PBS) containing 0.1 mg/mL BSA. Radioactivity was measured using a TopCount microplate scintillation counter. The activation of TRPA1 was measured by cellular uptake of radioactive calcium. The hypo-Osmolarity buffer-induced uptake was considered as 100%, and wells with normal radioactive assay buffer (300 mOsmol/L) were taken as 0%.

CYP Inhibition IC_{50} . Inhibition of CYP3A4 and 2D6 was determined as described.²⁴

Transport across MDCK Cells. Transport studies to determine apparent permeability and efflux ratios [efflux ratio = $P_{\text{app,B} \rightarrow \text{A}}/P_{\text{app,A} \rightarrow \text{B}}$] were performed in MDCK vector control or MDR1-transfected MDCK cells as described.²⁵

AITC Target Engagement Assay. The AITC target engagement assay was run according to the published procedure.²⁶

■ ASSOCIATED CONTENT

Supporting Information

The Supporting Information is available free of charge on the ACS Publications website at DOI: 10.1021/acs.jmedchem.6b00039.

TRPA1 potency data with standard deviations, CEREP panel data for compound 27, and computational method for predicting π -stacking interaction of 27 (PDF)
SMILES data for 27 (CSV)

■ AUTHOR INFORMATION

Corresponding Author

*E-mail: laurie.schenkel@amgen.com. Phone: 617-444-5244.

Notes

The authors declare no competing financial interest.

■ ACKNOWLEDGMENTS

The authors thank Loren Berry for plasma protein binding measurements, Virginia Berry and Xuhai Be for bioanalysis of the PK and PD studies, Jingzhou Liu for metabolite identification studies, Mary Wells for pharmacokinetic and drug metabolism studies, and Margaret Chu-Moyer for manuscript input.

■ ABBREVIATIONS USED

CFA, complete Freund's adjuvant; CDI, carbonyldiimidazole; DAST, diethylaminosulfur trifluoride; EDC, 1-ethyl-3-(3-(dimethylamino)propyl)carbodiimide; FLIPR, fluorometric imaging plate reader; PBS, phosphate-buffered saline; SIF, simulated intestinal fluid; T3P, propylphosphonic anhydride

■ REFERENCES

- (1) (a) Hinman, A.; Chuang, H.-H.; Bautista, D. M.; Julius, D. TRP channel activation by reversible covalent modification. *Proc. Natl. Acad. Sci. U. S. A.* **2006**, *103*, 19564–19568. (b) Macpherson, L. J.; Dubin, A. E.; Evans, M. J.; Schultz, P. G.; Marr, F.; Cravatt, B. F.; Patapoutian, A. Noxious compounds activate TRPA1 ion channels through covalent modification of cysteines. *Nature* **2007**, *445*, 541–545. (c) Bautista, D. M.; Movahed, P.; Hinman, A.; Axelsson, H. E.; Sterner, O.; Högestätt, E. D.; Julius, D.; Jordt, S.-E.; Zygmunt, P. M. Pungent products from garlic activate the sensory ion channel TRPA1. *Proc. Natl. Acad. Sci. U. S. A.* **2005**, *102*, 12248–12252.
- (2) Kwan, K. Y.; Glazer, J. M.; Corey, D. P.; Rice, F. L.; Stucky, C. L. TRPA1 modulates mechanotransduction in cutaneous sensory neurons. *J. Neurosci.* **2009**, *29*, 4808–4819.
- (3) Bandell, M.; Story, G. M.; Hwang, S. W.; Viswanath, V.; Eid, S. R.; Petrus, M. J.; Earley, T. J.; Patapoutian, A. Noxious cold ion channel TRPA1 is activated by pungent compounds and bradykinin. *Neuron* **2004**, *41*, 849–857.
- (4) Lee, S. P.; Buber, M. T.; Yang, Q.; Cerne, R.; Cortés, R. Y.; Sprou, D. G.; Bryant, R. W. Thymol and related alkyl phenols activate the hTRPA1 channel. *Br. J. Pharmacol.* **2008**, *153*, 1739–1749.
- (5) Bautista, D. M.; Pellegrino, M.; Tsunozaki, M. TRPA1: A gatekeeper for inflammation. *Annu. Rev. Physiol.* **2013**, *75*, 181–200.
- (6) Kwan, K. Y.; Glazer, J. M.; Corey, D. P.; Rice, F. L.; Stucky, C. L. TRPA1 modulates mechanotransduction in cutaneous sensory neurons. *J. Neurosci.* **2009**, *29*, 4808–4819.
- (7) McNamara, C. R.; Mandel-Brehm, J.; Bautista, D. M.; Siemens, J.; Deranian, K. L.; Zhao, M.; Hayward, N. J.; Chong, J. A.; Julius, D.; Moran, M. M.; Fanger, C. M. TRPA1 mediates formalin-induced pain. *Proc. Natl. Acad. Sci. U. S. A.* **2007**, *104*, 13525–13530.
- (8) Trevisani, M.; Siemens, J.; Materazzi, S.; Bautista, D. M.; Nassini, R.; Campi, B.; Imachi, N.; André, E.; Patacchini, R.; Cottrell, G. S.; Gatti, R.; Basbaum, A. I.; Bunnett, N. W.; Julius, D. J.; Geppetti, P. 4-Hydroxynonenal, an endogenous aldehyde, causes pain and neurogenic inflammation through activation of the irritant receptor TRPA1. *Proc. Natl. Acad. Sci. U. S. A.* **2007**, *104*, 13519–13524.
- (9) Eid, S. R.; Crown, E. D.; Moore, E. L.; Liang, H. A.; Choong, K.-C.; Dima, S.; Henze, D. A.; Kane, S. A.; Urban, M. O. HC-030031, a TRPA1 selective antagonist, attenuates inflammatory- and neuropathy-induced mechanical hypersensitivity. *Mol. Pain* **2008**, *4*, 48.
- (10) Petrus, M.; Peier, A. M.; Bandell, M.; Hwang, S. W.; Huynh, T.; Olney, N.; Jegla, T.; Patapoutian, A. A role of TRPA1 in mechanical hyperalgesia is revealed by pharmacological inhibition. *Mol. Pain* **2007**, *3*, 40.
- (11) Rooney, L.; Vidal, A.; D'Souza, A.-M.; Devereux, N.; Masick, B.; Boissel, V.; West, R.; Head, V.; Stringer, R.; Lao, J.; Petrus, M. J.; Patapoutian, A.; Nash, M.; Stoakley, N.; Panesar, M.; Verkuy, J. M.; Schumacher, A. M.; Petrassi, H. M.; Tully, D. C. Discovery, optimization, and biological evaluation of 5-(2-(trifluoromethyl)-phenyl)indazoles as a novel class of transient receptor potential A1 (TRPA1) antagonists. *J. Med. Chem.* **2014**, *57*, 5129–5140.
- (12) Kremeyer, B.; Lopera, F.; Cox, J. J.; Momin, A.; Rugiero, F.; Marsh, S.; Woods, C. G.; Jones, N. G.; Paterson, K. J.; Fricker, F. R.; villegas, A.; Acosta, N.; Pineda-Trujillo, N. G.; Ramirez, J. D.; Zea, J.; Burley, M.-W.; Bedoya, G.; Bennett, D. L.-H.; Wood, J. N.; Ruiz-Linares, A. A gain-of-function mutation in TRPA1 causes familial episodic pain syndrome. *Neuron* **2010**, *66*, 671–680.
- (13) Wheeler, S. E.; Houk, K. N. Substituent effects in the benzene dimer are due to direct interactions of the substituents with the unsubstituted benzene. *J. Am. Chem. Soc.* **2008**, *130*, 10854–10855.
- (14) Predicted interaction energies for compounds **9** and **14–19** were taken from ref **14** using the value for the corresponding substituted phenyl ring. The predicted interaction energy for **27** was calculated using the same method. See [Supporting Information](#).
- (15) Geometries were minimized by using B3LYP/6-31G* and overlaid using the quinazolinone cores.
- (16) See [Supporting Information](#).
- (17) Dib-Hajj, S. D.; Yang, Y.; Black, J. A.; Waxman, S. G. The Na_v1.7 sodium channel: from molecule to man. *Nat. Rev. Neurosci.* **2013**, *14*, 49–62.
- (18) (a) Ohkawara, S.; Tanaka-Kagawa, T.; Furukawa, Y.; Jinno, H. Methylglyoxal activates the human transient receptor potential ankyrin 1 channel. *J. Toxicol. Sci.* **2012**, *37*, 831–835. (b) Eberhardt, M. J.; Filipovic, M. R.; Leffler, A.; de la Roche, J.; Kistner, K.; Fischer, M. J.; Fleming, T.; Zimmermann, K.; Ivanovic-Burmazovic, I.; Nawroth, P. P.; Bierhaus, A.; Reeh, P. W.; Sauer, S. K. Methylglyoxal activates nociceptors through transient receptor potential channel A1 (TRPA1). *J. Biol. Chem.* **2012**, *287*, 28291–28306.
- (19) (a) Venkatachalam, K.; Montell, C. TRP Channels. *Annu. Rev. Biochem.* **2007**, *76*, 387–417. (b) Strotmann, R.; Harteneck, C.; Nunnenmacher, K.; Schultz, G.; Plant, T. D. OTRPC4, a nonselective cation channel that confers sensitivity to extracellular osmolarity. *Nat. Cell Biol.* **2000**, *2*, 695–702.
- (20) Copeland, K. W.; Boezio, A. A.; Cheung, E.; Lee, J.; Olivieri, P.; Schenkel, L. B.; Wan, Q.; Wang, W.; Wells, M. C.; Youngblood, B.; Gavva, N. R.; Lehto, S. G.; Geuns-Meyer, S. Development of novel azabenzofuran TRPA1 antagonists as in vivo tools. *Bioorg. Med. Chem. Lett.* **2014**, *24*, 3464–3468.
- (21) Chen, S.; Graceffa, R. F.; Boezio, A. A. Direct, regioselective N-alkylation of 1,3-azoles. *Org. Lett.* **2016**, *18*, 16–19.
- (22) Lee, K. J.; Wang, W.; Padaki, R.; Bi, V.; Plewa, C. A.; Gavva, N. R. Mouse monoclonal antibodies to transient receptor potential ankyrin 1 act as antagonists of multiple modes of channel activation. *J. Pharmacol. Exp. Ther.* **2014**, *350*, 223–231.
- (23) Klionsky, L.; Tamir, R.; Gao, B.; Wang, W.; Immke, D. C.; Nishimura, N.; Gavva, N. R. Species-specific pharmacology of trichloro(sulfanyl)ethyl benzamides as transient receptor potential ankyrin I (TRPA1) antagonists. *Mol. Pain* **2007**, *3*, 39.
- (24) Berry, L. M.; Zhao, Z. An examination of IC₅₀ and IC₅₀-shift experiments in assessing time-dependent inhibition of CYP3A4, CYP2D6 and CYP2C9 in human liver microsomes. *Drug Metab. Lett.* **2008**, *2*, 51–59.
- (25) Huang, L.; Berry, L.; Ganga, S.; Janosky, B.; Chen, A.; Roberts, J.; Colletti, A. E.; Lin, M. H. Relationship between passive permeability, efflux, and predictability of clearance from in vitro metabolic intrinsic clearance. *Drug Metab. Dispos.* **2010**, *38*, 223–231.
- (26) de Oliveira, C.; Garami, A.; Lehto, S. G.; Pakai, E.; Tekus, V.; Pohoczky, K.; Youngblood, B. D.; Wang, W.; Kort, M. E.; Kym, P. R.; Pinter, E.; Gavva, N. R.; Romanovsky, A. A. Transient receptor potential channel ankyrin-1 is not a cold sensor for autonomic thermoregulation in rodents. *J. Neurosci.* **2014**, *34*, 4445–4452.